ChemMedChem

Chemistry Europe
European Chemical Societies Publishing

Accepted Article

Title: Recent Drug Development and Medicinal Chemistry Approaches for the Treatment of SARS-CoV-2 and Covid-19

Authors: Arun K Ghosh, Jennifer L. Mishevich, Andrew Mesecar, and Hiroaki Mitsuya

To be cited as: *ChemMedChem* **2022**, e202200440

Link to VoR: https://doi.org/10.1002/cmdc.202200440

WILEY-VCH

10.1002/cmdc.202200440

WILEY-VCH

REVIEW

Recent Drug Development and Medicinal Chemistry Approaches for the Treatment of SARS-CoV-2 and Covid-19

Arun K. Ghosh,*[a,b] Jennifer L. Mishevich,[a,b] Andrew Mesecar,[a,c,d] and Hiroaki Mitsuya[e,f,g]

WILEY-VCH

REVIEW

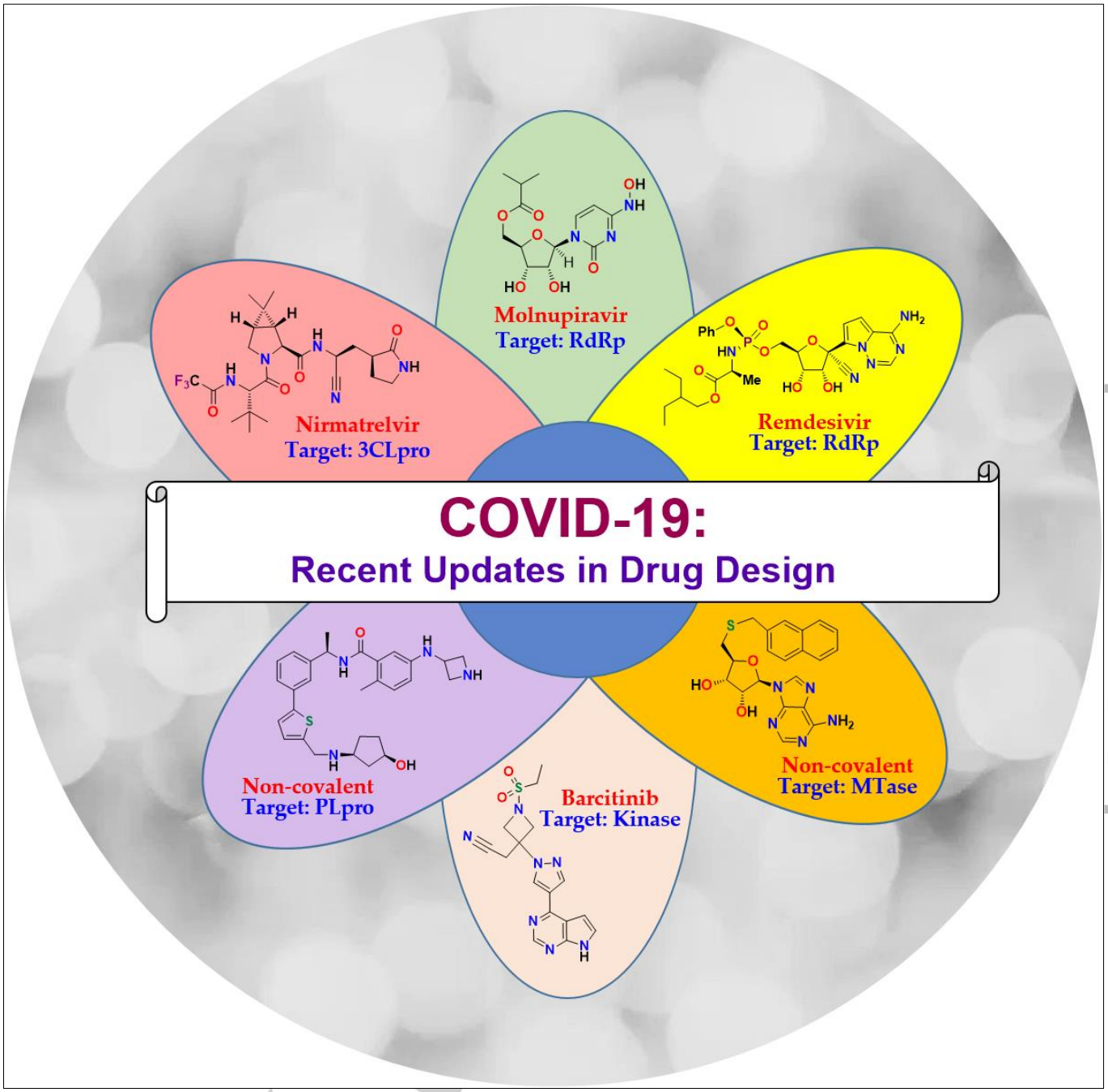

[a] Professor A. K. Ghosh, Ms. J. Mishevich, Professor A. D. Mesecar
Department of Chemistry
Purdue University
West Lafayette, IN 47907
akghosh@purdue.edu
[b] Professor A. K. Ghosh, Ms. J. Mishevich
Department of Medicinal Chemistry and Molecular Pharmacolgy
Purdue University
West Lafayette, IN 47907
[c] Professor A. D. Mesecar
Department of Biological Sciences
Purdue University
West Lafayette, IN 47907, USA
[d] Professor A. D. Mesecar
Department of Biochemistry
Purdue University
West Lafayette, IN 47907
[e] Dr. H. Mitsuya
Departments of Hematology and Infectious Diseases
Kumamoto University School of Medicine
Kumamoto 860-8556, Japan
[f] Dr. H. Mitsuya
Experimental Retrovirology Section
HIV and AIDS Malignancy Branch
National Cancer Institute
Bethesda, MD 20892
[g] Dr. H. Mitsuya
Center for Clinical Sciences
National Center for Global Health and Medicine
Shinjuku, Tokyo 162-8655, Japan

Abstract: COVID-19, caused by SARS-CoV-2 infection, continues to be a major public health crisis around the globe. Development of vaccines and the first cluster of antiviral drugs has brought promise and hope for prevention and treatment of severe coronavirus disease. However, continued development of newer, safer, and more effective antiviral drugs are critically important to combat COVID-19 and counter the looming pathogenic variants. Studies of the coronavirus life cycle revealed several important biochemical targets for drug development. In the present review, we focus on recent drug design and medicinal chemistry efforts on small molecule drug discovery including the development of nirmatrelvir that targets viral protein synthesis and remdesivir and molnupiravir that target viral RdRp. These are recent FDA approved drugs for the treatment of COVID-19.

1. Introduction

Severe acute respiratory syndrome coronavirus 2 (SARS-CoV-2) originated in Wuhan, China in late December 2019.[1,2] This outbreak began spreading at an alarming rate, and unleashed a severe health crisis around the globe. Subsequently, the uncertainties caused a serious economic meltdown worldwide. On March 11, 2020, the World Health Organization (WHO) declared the novel coronavirus (COVID-19) outbreak a global pandemic.[3,4] Since then, it has gone on to affect millions of lives across the globe and caused nearly 6.3 million deaths as of June 7, 2022.[5] Human-human transmission for SARS-CoVs occurs primarily via respiratory droplets through sneezing, coughing, or close contact between persons. Mild symptomatic cases may include: fever, fatigue, dyspnea.[6] More severe cases of SARS-CoV-2 develop pneumonia, acute respiratory distress, and hypoxia.[6] Early on, many laboratories around the world got involved in the development of COVID-19 therapeutics. These include, development of therapies through drug repurposing, monoclonal antibody-based treatment, convalescent plasma therapies, vaccine therapies, and target-based drug development.[7,8] We will focus our review on recent efforts and updates on new drug development since our prior review in 2020.[9]

Coronaviruses are the largest known single stranded RNA viruses that infect animals and humans leading to respiratory, gastrointestinal, hepatic, and neurologic diseases.[10] There are currently four different genera of human coronaviruses (HCoVs): alpha-coronavirus, beta-coronavirus, gamma-coronavirus, and delta-coronavirus. SARS-CoV-2 is the seventh human coronavirus. Another six have been identified: alpha-CoVs-NL63 and HCoVs-229E, and beta-CoVs HCoVs-OC43, HCoVs-HKU1, severe acute respiratory syndrome-CoV (SARS-CoV-1), and Middle East respiratory syndrome-CoV (MERS-CoV). These have been reviewed extensively.[11] Recently, a newly identified alpha-coronavirus was identified in patients hospitalized with pneumonia.[12] This new human coronavirus turns out to be a novel "canine-feline coronavirus" that is called CCoV-human pneumonia (HuPn)-2018, and additional studies have now turned up even more of these hybrid alpha-coronaviruses around the globe.[12] Sequence analysis suggests that these are novel canine-feline-porcine-like (CFPL) CoVs of Alphacoronavirus 1 species that can infect humans (hCFPL-CoVs) and are associated with acute respiratory illness.

The first SARS outbreak (SARS-CoV-1) originated in the Guandong Province, China in 2002.[13,14] It spread to several Asian countries, North America, and Europe. However, it was promptly contained and affected more than 8,000 individuals with 774 deaths and a 10% mortality rate.[15,16] There is a 82% genome similarity between SARS-CoV-1 and SARS-CoV-2 and a 90% resemblance in many essential enzymes. With the arrival of

Arun K. Ghosh received his BS and MS in Chemistry from the University of Calcutta and Indian Institute of Technology, Kanpur, India, respectively. He obtained his Ph.D. in chemistry from the University of Pittsburgh (1985). He then pursued out postdoctoral research in Professor E. J. Corey's laboratory at Harvard University (1985-1988). He was a research fellow at Merck before to joining the chemistry faculty at the University of Illinois, Chicago as an assistant Professor in 1994. In 2005, he joined the Department of Chemistry and Medicinal Chemistry at Purdue University, West Lafayette. In 2009, he became the Ian P. Rothwell Distinguished Professor of Chemistry and Medicinal Chemistry. His research interests are in broad areas of synthetic organic, structure-based drug design, and medicinal chemistry.

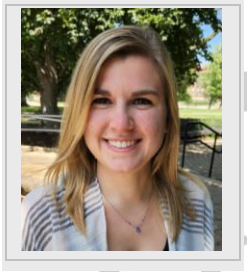

Jennifer L. Mishevich is a graduate student in the department of chemistry at Purdue University. She obtained her Bachelor of Science degree from Indiana University Northwest where she worked in the laboratory of Professor Walker on the synthesis of NS containing ligands. She then went on to graduate school and joined Professor Ghosh's laboratory in 2018 where she began pursuing her PhD in organic chemistry. Her current research focuses on the design, synthesis, and biological evaluation of next generation HIV protease inhibitors and drug design for severe acute respiratory syndrome coronavirus 2 (SARS-CoV-2).

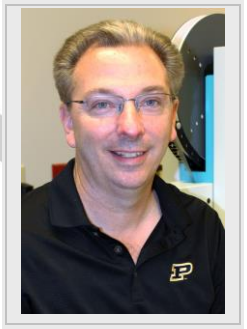

Andrew D. Mesecar received his B.S. in Chemistry from Purdue University in 1988 and his Ph.D. in Biochemistry in 1995 from the University of Notre Dame. He pursued post-doctoral research at UC. Berkeley (1995-1999) under the direction of Prof. Daniel E. Koshland Jr. He joined the faculty in Medicinal Chemistry & Pharmacognosy at the University of Illinois-Chicago as an assistant professor in 1999 and was promoted to full Professor in 2008. In 2010, he was recruited to Purdue as the Walther Professor of Structural Biology and Deputy Director of the Purdue Center for Cancer Research. He is interested in the structure and function of medically important enzymes involved in cancer, coronavirus infections and Alzheimer's disease, and using structure-based approaches to design therapeutics against these enzymes.

Hiroaki Mitsuya received his M.D. and Ph.D. from National Kumamoto University School of Medicine, Japan. Following training as an oncologist/hematologist/immunologist, he joined the National Cancer Institute in 1982. Dr. Mitsuya has been Principal Investigator & Chief, Experimental Retrovirology Section, National Cancer Institute, Bethesda, Maryland since 1991. Since 1997, Dr. Mitsuya has also served as Professor of Medicine and Chairman, Departments of Hematology, Clinical Immunology/Rheumatology, and Infectious Diseases in Kumamoto University School of Medicine.

SARS-CoV-1, there was significant medicinal chemistry efforts geared toward developing concepts and strategies to block SARS-CoV-1 replication and to develop target-based therapeutics. Indeed, much of the ground work for blocking essential enzyme functions provided insights and a head start for the development of mechanism-based drugs against SARS-CoV-2 infection and COVID-19.[17,18,19,20] We will highlight here recent developments and approaches to SARS-CoV-2 and Covid-19 therapeutics.

2. Drug design Targets that block Viral Replication

SARS-CoV-2 binds to the host cell surface receptor, angiotensin-converting enzyme 2 (ACE2) to enter the cell. After cell entry, viral RNA attaches to the host cell ribosome to produce two polyproteins, pp1a and pp1ab, which are subsequently cleaved by the coronavirus main protease, or 3-chymotrypsin-like protease (3CLpro), and papain-like protease (PLpro).[21,22] Cleavage of these polyproteins leads to the formation of several essential enzymes such as RNA-dependent RNA polymerase (RdRp), which is responsible for genome replication.[23] As shown in Figure 1, many of these enzymes have all been subjected to intensive research as targets for SARS-CoV antiviral therapies.

Two main targets for antiviral therapies are two cysteine proteases, PLpro and 3CLpro, also known as the main protease (Mpro).[24,25] Both proteases are responsible for processing 16 nonstructural proteins (nsps), which are essential for viral replication and maturation.[26,27,28] The sequence identity for 3CLpro between SARS-CoV-1 and SARS-CoV-2 is 96%. 3CLpro is responsible for cleaving the polyprotein and generating functional viral proteins such as: RdRp, RNA binding proteins, exoribonuclease, helicase, and methyltransferase.[29] 3CLpro is active as a homodimer and contains a catalytic dyad of Cys-His, whereas PLpro has a catalytic triad of Cys-His-Asp.[30] PLpro has an 83% sequence identity similarity between SARS-CoV-1 and SARS-CoV-2. PLpro is responsible for processing the replicase polyprotein and removing cellular substrates such as ubiquitin, termed deubiquitylation, and interferon-stimulated gene product 15 from host cell proteins.[31,32] This allows the virus to escape the

host innate immune system. Other important drug design targets for COVID-19 treatment include, the spike/ACE2 viral attachment, cell entry, viral helicase, replication complex, nucleocapsid, viral RdRp, and methyltransferase. Many of these areas are undergoing active research and we will highlight recent developments.

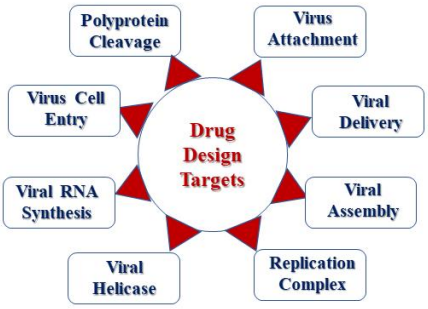

Figure 1. Important biochemical targets for COVID-19 drug discoveries.

3. Currently Approved Drugs for treatment of COVID-19

Since the first SARS-CoV-1 outbreak in 2003 and later with the MERS-CoV outbreak, much effort was devoted to drug repurposing.[33,34] The outbreak of COVID-19 led to significant activity in this area due to the overwhelming situation and urgency for treatment. A major advantage of drug repurposing is that the drug is already approved for use in one area, therefore drug safety and pharmacokinetic properties are well established. As a result, clinical trials can be conducted directly in patients, leading to accelerated approval if efficacy is observed. Many approved drugs have been reported to block SARS-CoV-2 replication.[7,8] Several of these drugs have undergone clinical trials for potential treatment of SARS-CoV-2 infection and COVID-19. These include, remdesivir (**1**, Figure 2) which was initially developed for treatment of hepatitis C infection, chloroquine and hydroxyl-chloroquine which were developed for treatment of malaria, favipiravir which was developed as an anti-influenza drug, and masitinib which was developed as a kinase inhibitor against mast cell tumors in animals. Among these, only remdesivir (**1**), developed by Gilead Sciences, was initially approved by the FDA for treatment of COVID-19 patients.[35,36] Remdesivir's biological mechanism of action involves interfering with genome replication by targeting RdRp.[37,38] Structurally, remdesivir resembles adenosine and gets incorporated into nascent viral RNA, which causes premature termination of the viral RNA chain. Remdesivir was approved as an intravenous drug that must be administered in a health care setting. However, clinical efficacy of remdesivir has remained inconclusive.[39,40] One of the reasons for this controversy is that the clinical trial was conducted on severe COVID-19 patients and antiviral drugs may not have been useful at that stage of infection. A recent clinical trial of remdesivir for treatment of mild COVID-19 patients showed higher efficacy.[41,42] It is now generally accepted that antiviral drugs for COVID-19 treatment should be administered in the earliest viral replication phase. Molnupiravir (FIDD-2801), a nucleoside analog, developed by Merck Research Laboratories, was recently given emergency use authorization (EUA) by the US FDA in 2021 as an

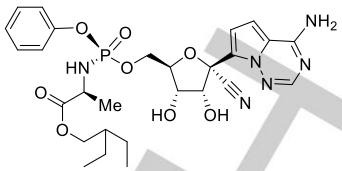

Remdesivir (1)
Target: RdRp inhibitor
Injection drug

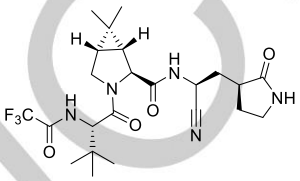

Nirmatrelvir (PF-07321332) (2)
Target: SARS-CoV-2-3CLPro inhibitor
Oral drug

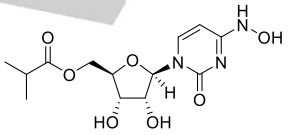

Molnupiravir (EIDD-2801) (3)
Target: RdRp inhibitor
Oral drug

Figure 2. Currently available COVID-19 Drug Therapies**.**

oral drug.[43,44] Molnupiravir has the same mechanism as remdesivir. It is an RdRp inhibitor, originally developed for treatment of viral infection caused by RNA viruses. One of the main advantages of oral drugs is that the patients can be prescribed antiviral drugs at the earliest indication without hospitalization. Early phase 3 clinical trials with COVID-19 patients showed about 50% reduction in hospitalization compared to the placebo group with no reported deaths.[44,45]

Paxlovid (PF-07321332), developed by Pfizer, was recently granted EUA by the FDA in 2021 as an oral drug for treatment of COVID-19 patients.[46,47] The biological mechanism of action involves inhibition of viral protease (3CLpro or Mpro) which plays a critical role in the viral replication cycle by cleaving viral proteins and producing essential individual, mature proteins necessary for viral replication.[24,25] Many inhibitors of 3CLpro were initially developed for treatment of SARS-CoV-1 during the outbreak in 2003-2004.[9,25,48] The Phase II-III data of Paxlovid clinical trials showed that treatment of patients within three days of COVID-19 symptoms reduced COVID related hospitalization by 89% compared to the placebo group.[46,49] There are many other drug discovery targets being actively investigated for development of effective COVID-19 therapeutics. The major targets and progress in these areas will be discussed in the following section.

4. SARS-CoV-2 Protease Inhibitors for COVID-19 treatment

Viral proteases are considered excellent drug design targets due to their involvement in virus maturation and production of essential functional proteins. Indeed, protease inhibitor drugs play

critical roles in the treatment of chronic viral infections, such as HIV/AIDS, hepatitis C virus, hepatitis B virus, herpesvirus and influenza virus.[50,51,52] Since the SARS-CoV-1 outbreak in 2003 and MERS-CoV outbreak in 2012, SARS-CoV-1 3CLpro and SARS-CoV-1 PLpro became very attractive targets for drug discovery and early development of peptidomimetic and small molecule SARS-CoV-1 protease inhibitors.[9,25,48] The in vivo efficacy of 3CLpro inhibitors in mice and feline species has been documented prior to the development of paxlovid.[53,54] As the activity of 3CLpro and PLpro are essential for coronavirus replication, an intense effort towards protease inhibitor design and development has commenced with the COVID-19 pandemic. We will discuss recent updates of SARS-CoV-2 3CLpro and PLpro inhibition design in this section.

4.1 SARS-CoV-2 3CLpro Inhibitors

Of the two main proteases, SARS-CoV-2 3CLpro is the most-well characterized.[55,56] Several different types of inhibitors have been investigated including peptidomimetic covalent inhibitors, small molecule covalent inhibitors, and noncovalent inhibitors.[9,57] Historically, covalent inhibitors were thought to be generally cytotoxic due to off target effects; however, recent developments have shown that this is not always the case. Development of covalent cysteine proteases has shown significant potential for SARS-CoV-2 drug development. Several different classes of protease inhibitors will be discussed in this section including peptidomimetic covalent inhibitors, small molecule covalent inhibitors, and noncovalent inhibitors.

4.1.1 Peptidomimetic Covalent 3CLpro Inhibitors

The development of early peptidomimetic SARS-CoV-1 3CLpro inhibitors has been reviewed previously.[9,48,57] Structural evolution of 3CLpro inhibitors started with the design of covalent inhibitor **4** (Figure 3) with an α,β-unsaturated ester, Michael acceptor warhead.[58,59] Inhibitor design also evolved to reversible inhibitors like the phthalhydrazido-methyl ketone warhead in inhibitor **5**, and benzothiazolyl ketone-derived inhibitors **6** and **7**.[25,60] Inhibitor **7** with a P3 indole methoxy group was synthesized and evaluated against SARS-CoV-2 3CLpro.[61] Compound **7** is a tight binding reversible covalent inhibitor and showed a K_i value of 17.6 nM against SARS-CoV-2 3CLpro. The compound displayed an antiviral EC_{50} value of 4.2 μM in VeroE6 cell-based assay with RNA-qPCR. Its apparent cytotoxic CC_{50} value was >100 μM. Interestingly, inhibitor **7** when combined with remdesivir, an RdRp inhibitor, exerted synergistic activity against SARS-CoV-2 and viral breakthrough did not occur. At 2 μM remdesivir and 2 μM inhibitor **7** viral replication was suppressed by 0.67-fold and 1.3-fold, respectively. When both compounds were combined, the suppression was 1.8-fold. At 10 μM remdesivir and 10 μM inhibitor **7** results showed viral suppression to be 20-fold and 210-fold, respectively. However, when combined, that suppression was 590,000-fold. At 20 μM remdesivir and 20 μM inhibitor **7** viral suppression was 1,600,000-fold.[61]

The X-ray structure of SARS-CoV-2 3CLpro and inhibitor **7** complex was determined and the structure gave molecular insight into the inhibitor-protease interactions. The active site inhibitor-bound structure is shown in Figure 4. As can be seen, the sulfur atom of Cys145 forms a covalent bond with the carbonyl carbon next to the benzothiazole of compound **7**, resulting in the formation of a tetrahedral intermediate. The hemiacetal alcohol forms one direct hydrogen bond and water-mediated hydrogen bond interactions around the oxyanion hole residues, Cys145 and

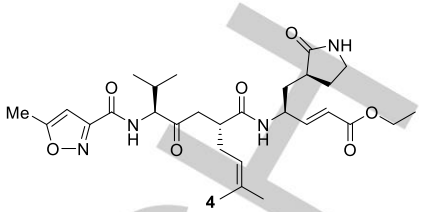

4
K_i = 0.014 min^{-1}
IC_{50} (3CLpro) = 70 μM

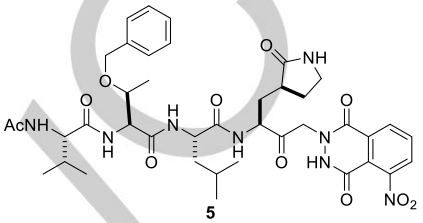

5
IC_{50} = 0.60 μM (SARS-Cov-1 3CLpro)

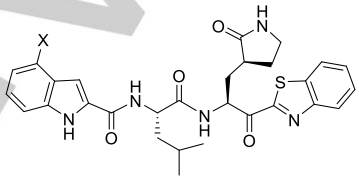

6 (X = H)
K_i = 0.065 μM (SARS-Cov-1 3CLpro)

7 (X = OMe)
K_i = 65 nM (SARS-Cov-1 3CLpro)
K_i = 17.6 nM (SARS-CoV-2 3CLpro)
EC_{50} = 4.2 μM (antiviral, SARS-CoV-2)

Gly143. The P3 indole amide carbonyl

Figure 3. Structure of SARS-CoV 3CLpro inhibitors **4-7.**

and amide NH form two hydrogen bonds linking the main chain carbonyl and the amide group of Glu166. The side chain oxygen of Gln-189 forms hydrogen bonds with P2 amide carbonyl and NH groups. The lactam carbonyl of inhibitor **7** forms a hydrogen bond with His163 side chain. The structure also shows several hydrophobic residues contribute to binding affinity via van der Waals interactions. The distal benzene ring of the benzothiazole is sandwiched by Leu27 and Met49 in the S2 sub-pocket.[61]

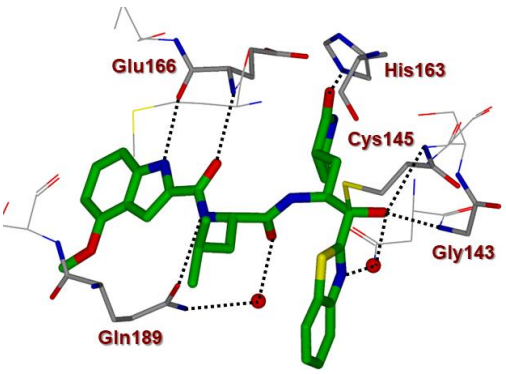

Figure 4. X-ray structure of SARS-CoV-2 3CLpro and inhibitor 7 complex (PDB: 7JKV)

Bisulfite derivative, GC-376 (**8**, Figure 5) has been shown to potently inhibit SARS-CoV-2 3CLpro.[62,63] GC-373 (**9**) was initially developed to inhibit feline infectious peritonitis virus (FIVP), a fatal infection in cats caused by mutations of feline enteric coronavirus (FECV).[53] GC-376 is the prodrug of aldehyde inhibitor GC-373, and it was shown to exhibit in vivo efficacy in treating certain forms of FIVP.[53] With the outbreak of COVID-19, there has been much research into GC-373 and its derivatives. Vuong et. al. and others have shown that GC-373 inhibits SARS-CoV-2 3CLpro with a K_i value of 150 nM and antiviral activity of 700 nM.[64,65] Structural modifications were carried out to further improve activity. Derivatives **10** and **11** were shown to inhibit SARS-CoV-2 3CLpro more potently, however, their antiviral activity was not reported.[66]

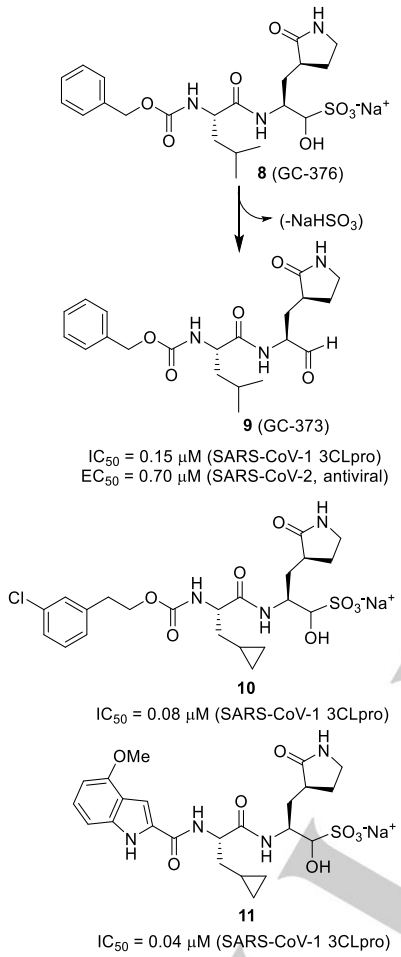

Figure 5. Structure of SARS-CoV 3CLpro inhibitors **8-11.**

The X-ray structure of GC-376-bound SARS-CoV-2 3CLpro has been determined. As shown in Figure 6, the structure revealed that Cys145 forms a covalent bond with the aldehyde functionality and forms a hemithioacetal.[65,66] The P1 lactam carbonyl forms a hydrogen bond with His163 and the lactam NH forms a hydrogen bond with the side chain carboxylic acid of Glu166. The P2 isobutyl group fits in the S2 pocket surrounding Arg40, His41, and Asp187.

Repurposing of previously approved protease inhibitors for the treatment of COVID-19 has been conducted in many laboratories.[7,8] This led to the identification of many drug candidates. However, there was wide variation in assay results.

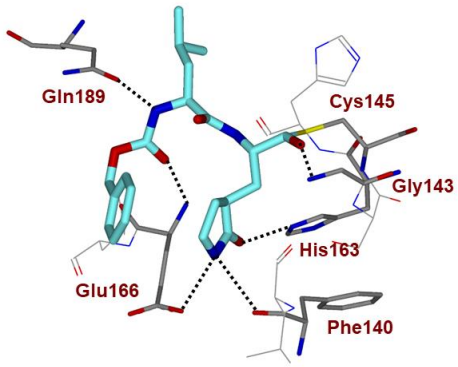

Figure 6. X-ray structure of SARS-CoV-2 3CLpro and GC-376 complex (PDB: 6WTK)

Among the most promising outcome is the identification of HCV NSP3 protease inhibitor drugs boceprevir **12** (Figure 7) and telaprevir **13**.[65,67] Both drugs are potent peptidyl inhibitors of HCV NSP3, which is a serine protease.[68,69] Both compounds have been shown to inhibit SARS-CoV-2 Mpro from several labs.[65,67] However, inhibition data show wide variability. Like other peptidomimetic inhibitors of 3CLpro, these serine protease inhibitor drugs possess the same α-ketoamide warhead. Like the ketobenzothiazole warhead in compound **7**, the ketoamide functionality forms a covalent bond with Cys145 in the active site. Boceprevir, **12**, has inhibited SARS-CoV-2 3CLpro with an IC_{50} range of 1.6 μM to 8 μM. In contrast, teleprevir showed weak inhibition with an IC_{50} value of 56 μM. Boceprevir antiviral activity EC_{50} value was determined to be 15.6 μM with remdesivir as a positive control and an EC_{50} value of 0.58 μM. Teleprevir showed marginal antiviral activity.[65,67,70] Structurally, boceprevir possesses a P1β-cyclobutylalanyl group and teleprevir contains a norleucine moiety. Other key features include a P2 dimethylcyclopropyl proline for boceprevir and a bicyclic cyclopentyl fused proline derivative for teleprevir. Both drugs contain a P3-tert-butyl glycine ligand.

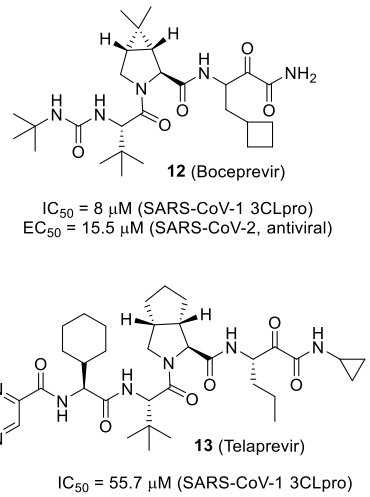

Figure 7. Structure of HCV NSP3 and SARS-CoV 3CLpro inhibitors, boceprevir **(12)** and telaprevir **(13)**.

The first X-ray crystal structure of SARS-CoV-2 3CLpro bound to boceprevir was determined by our group early in the

COVID-19 pandemic and was released via the PDB (6WNP).[70] The X-ray crystal structures of boceprevir and teleprevir bound to SARS-CoV-2 3CLpro were also determined by others.[65,70] Structural analysis of boceprevir-bound 3CLpro is shown in Figure 8. Cys145 forms a covalent bond with the ketoamide warhead and subsequently forms a thiohemiacetal moiety. The resulting hydroxyl group forms a hydrogen bond with the His41 side chain and stabilizes the oxyanion hole. The P1 cyclobutylmethyl group occupies the shallow S1 pocket. The backbone of His164 and Glu166 forms important hydrogen bonds with the main chain of boceprevir. The X-ray structure of boceprevir-bound and teleprevir-bound 3CLpro are being utilized for improving drug-like properties, structures and antiviral activity against SARS-CoV-2 3CLpro. These are highlighted in the following section.

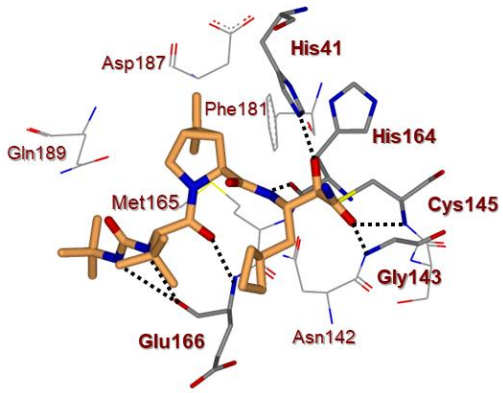

Figure 8. X-ray structure of the SARS-CoV-2 3CLpro-boceprevir (**12**) complex determined to 1.45 Å (PDB: 6WNP)

Based upon boceprevir or telaprevir-bound X-ray structures, a number of bicycloproline derived inhibitors have been prepared and evaluated by Yang and collaborators.[71] As shown in Figure 9, previously optimized, the P1 lactam was maintained as a fixed substituent in compound **14**. The P2 proline derivative of boceprevir and the bicyclic telaprevir ligand have been introduced in combination with a small electrophilic aldehyde warhead. This P1 moiety is the active pharmacophore, which forms a covalent bond with Cys145. Unfortunately, the extremely reactive nature of the aldehyde raises some clinical safety concerns for these inhibitors. The γ-lactam mimics the native P1 glutamine structure and fills the S1 subsite, and hydrophobic, medium sized subgroups were utilized in the P3 position to enhance the potency and pharmacokinetic properties.[71] All compounds were tested for their biological activity against SARS-CoV-2 3CLpro in a FRET assay. IC_{50} values were found to be in the low nanomolar range (from 7.6 to 748 nM), for compounds **14**-**16**.

The crystal structure of **16**-bound to SARS-CoV-2 3CLpro was determined. As shown in Figure 10, a covalent bond is formed between the aldehyde carbonyl carbon and the sulfur on Cys145. Two hydrogen bonds between the aldehyde carbonyl oxygen and the backbone amides of Cys145 and Gly143 can be observed. The bicycloproline extends into the S2 pocket where it forms hydrophobic interactions with the pocket residues. The P3 portion interacts with the amide backbone of Glu166 and the extended conformation of ethyl-3,5-difluorobenzene side chain extends into the S4 subsite.

Several compounds showed nanomolar or low micromolar EC_{50} values (range between 0.53 and 30.5 μM).[71] Interestingly, some compounds with high potency in the enzymatic assay exhibited only marginal activity in the antiviral assay. This was

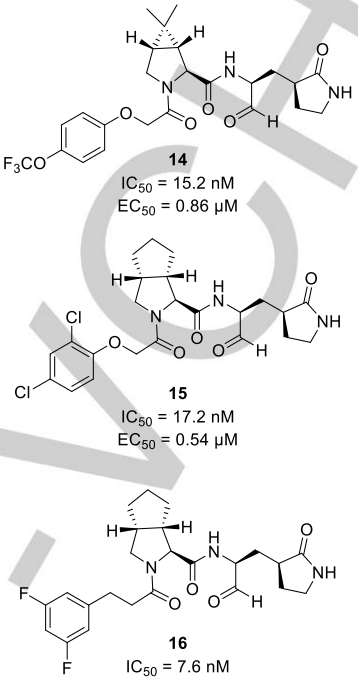

Figure 9. Bicycloproline Inhibitors.

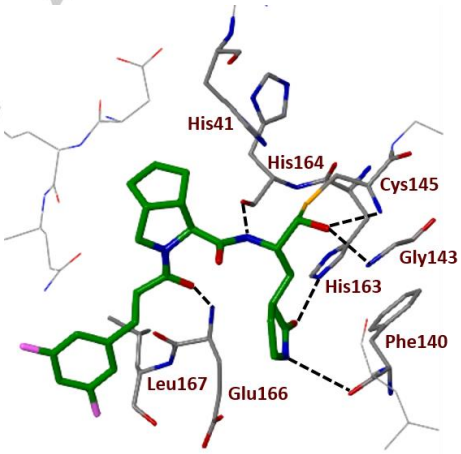

Figure 10. X-ray Structure of **16** with 3CLpro (PDB 7D3I).

proposed to be caused by low lipophilic properties of certain P3 ligands, resulting in poor cell membrane permeability. This class of compounds displayed no cytotoxicity in any of the cell lines tested including, Vero E6, HPAEpiC, LO2, BEAS-2B, A549, and Huh7 cells. Preliminary pharmacokinetic property experiments were performed to determine which compounds would be good for in vivo antiviral studies. Compounds **14** and **15** showed oral bioavailabilities of 11.2% and 14.6%, respectively.[71] In vivo tests were performed on mice in which both **14** and **15** were utilized, and it was found that the treatment group contained lower mean viral RNA loads in lung tissues than those of the control group. Recent investigations by Liu and co-workers into boceprevir based derivatives determined that a P4 N-terminal carbamate

improves activity and that an O-tert-butyl-threonine P3 ligand allows compounds to achieve higher cellular and antiviral activity.[72] Other recent investigations into α-ketoamide warhead containing 3CLpro inhibitors have culminated in lead compounds with good activity and oral bioavailability against several SARS-CoV-2 variants.[73]

Based upon similar studies mentioned above, Xia and co-workers reported peptidomimetic covalent inhibitors **17** and **18** shown in Figure 11.[74] Inhibitor **17** is a hybrid of GC-376 (**8**) and telaprevir and compound **18** is a hybrid of **8** and boceprevir. These inhibitors displayed potent enzymatic inhibition against SARS-CoV-2 3CLpro as well as several other coronaviruses. In a FRET assay both inhibitors had similar potency to **8**, although **18** was the more potent compound based on their in house designed Flip-GFP Mpro assay.[74] Antiviral activities were determined using immunofluorescence assay in VeroE6 and Caco2-ACE2 cell lines. Compound **18** showed an EC_{50} value of 0.37 µM in Vero E6 cells. Inhibitor **18** also had antiviral activity in Caco2-ACE2 cells with an EC_{50} of 1.06 µM compared to inhibitor **17** at 5.24 µM, and lead compound **8** at 2.9 µM. Both derivatives inhibited 3CLpro in other coronaviruses such as, SARS-CoV, MERS-CoV, HCoV-OC43, HCoV-NL63, and HCoV-229E in the FRET-based enzymatic assay. Inhibitor **17** had improved selectivity compared to the control compound against host cysteine proteases calpain I and cathepsin L.[74]

Selectivity was tested for each compound against cathepsin L, calpain I, cathepsin K, caspase-3, and serine protease trypsin. It was found that **8** was a potent inhibitor of calpain I and cathepsin L. Inhibitors **17** and **18** displayed significantly reduced inhibition of the off-target enzyme.[74] Lead compound **8** was also a potent inhibitor for cathepsin K, and while both designed inhibitors had reduced inhibitory activity, they also were quite potent against the off-target enzyme. A crystal structure of inhibitor **18** bound SARS-CoV-2 3CLpro determined the active site interactions, including formation of covalent bond with Cys145 is shown in Figure 12.

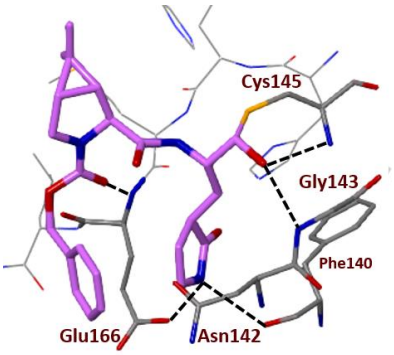

Figure 12. Peptidomimetic Inhibitor **18** bound 3CLpro (PDB 7LYI).

Bai and co-workers reported a series of peptidomimetic SARS-CoV-2 3CLpro inhibitors with α -acyloxymethylketone lactam as the glutamine mimetic.[75] Representative inhibitors **19-21** are shown in Figure 13. The design work stemmed from studies of Krantz and co-workers, who reported related work which involved design of inactivators of cysteine proteases like cathepsin B.[76,77] In particular, this earlier work examined leaving groups at the α-position of an α-substituted methyl ketone. It was observed that the pK_a of the leaving group correlated with the irreversible, covalent interaction. The choice of the α-leaving group is important as chloromethyl ketones are too reactive and cytotoxic.

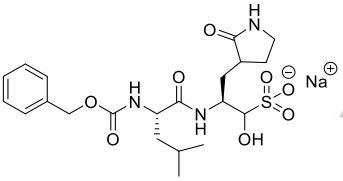

8
IC_{50}= 0.041 µM
EC_{50}= 0.96 µM

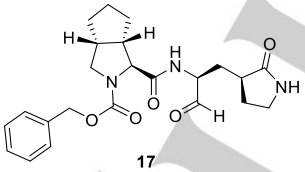

17
IC_{50} = 0.051 µM
EC_{50} = 2.56 µM

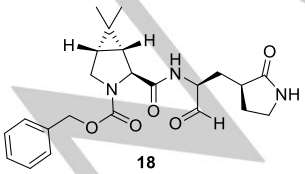

18
IC_{50} = 0.054 µM
EC_{50} = 0.37 µM

Figure 11. Peptidomimetic covalent inhibitors

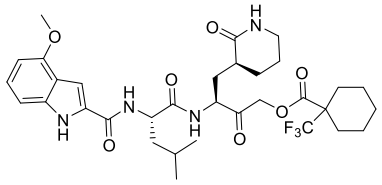

19
IC_{50} = 86.3 nM
EC_{50} = 0.6 µM

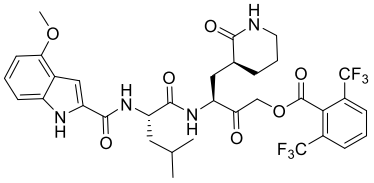

20
IC_{50} = 1 nM
EC_{50} = 0.16 µM

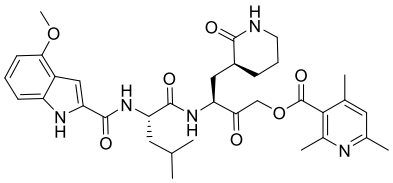

21
IC_{50} = 19 nM
EC_{50} = 0.3 µM

Figure 13. Peptidomimetic α-acyloxymethylketone Inhibitors

Fluoromethyl ketone is more selective, but it may also generate toxic metabolites.[78,79] Krantz and co-workers previously utilized benzoate esters and a few aliphatic esters of hydroxymethyl ketones as inactivators of cysteine proteases. Results indicated 2,6-bistrifluoromethyl and 2,6-dichloro benzoates as potent irreversible inactivators.[76,77] Based upon the results of diphenylphosphinyl, tretronoyl, and peptidyl esters, an α-acyloxy group was examined. This allows for pK_a adjustments to balance the rapid irreversible adduct formation and excessive reactivity that sequester glutathione or cause cytotoxicity.

Heteroaromatic rings were incorporated to allow more polar surfaces to increase solubility and reduce molecular planarity based upon previous studies. Steric hinderance around the ester was introduced to slow hydrolysis and increase stability. The P2 4-methoxyindole and leucine were left unchanged throughout the SAR study.[75] The six-membered lactam was also explored compared to the standard 5-membered lactam for further investigation in the S1 pocket. This was found to not have a significant effect on inhibitory activity. Variation of the ester moiety to contain an electron-withdrawing group was also explored in order to reduce the pK_a of the corresponding acid leaving group. This phenomenon was exemplified with inhibitor **19**, which displayed an enzyme IC_{50} value of 86 nM.[75] Inhibitor **20** displayed very potent enzyme inhibitory activity with IC_{50} value of 1 nM. Substituted pyridinyl derivatives such as in compound **21** were less potent than pyridine alone, but more potent than **8**.

Antiviral activity was observed at low micromolar range, including compounds **20** and **21** and no toxicity was observed up to 200 μM. Inhibitor **19** had good potency and plasma stability.[75] These compounds show antiviral activity against other coronavirus strains. The X-ray crystal structure of the inhibitor **21**-bound to SARS-CoV-2 3CLpro was determined. As shown in Figure 14, Cys145 formed a covalent linkage with the inhibitor and ester carbonyl turned into a thioether functionality.

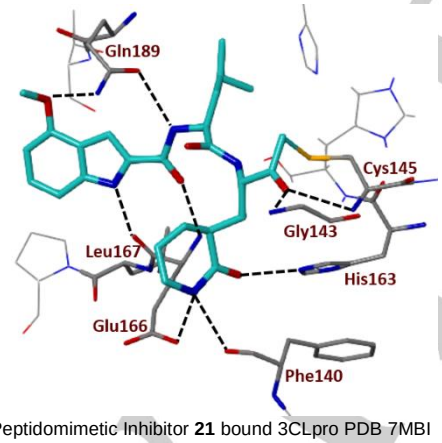

Figure 14. Peptidomimetic Inhibitor **21** bound 3CLpro PDB 7MBI

Hoffman and co-workers also investigated peptidomimetic covalent inhibitors with hydroxymethyl ketone and derivatives as warheads.[80] This class of compounds were initially developed during the first SARS outbreak in 2003. Following the COVID-19 outbreak, investigators examined hydroxymethyl ketone **22** (Figure 15) and its derivatives as potential therapeutics for COVID-19 treatment. The antiviral activity of compound **22** was evaluated against a panel of human viruses. Compound **22** does not inhibit human rhinovirus strains HRv-14 and HRv-16, HIV-1, HCMV in cell culture. Also, it does not inhibit HCV replication. The X-ray structural studies of **22**-bound to the 3CLpro of SARS-CoV-1 and CoV-2 were determined. The ligand binding sites are nearly identical. Also, as expected, the hydroxymethyl ketone carbonyl carbon formed a covalent bond to the 3CLpro active site Cys145 and generated a tetrahedral carbinol complex as shown in Figure 16. Compound **22** was tested for its SARS-CoV-2 3CLpro and antiviral activity. It was found that **22** has acceptable solubility, stability in plasma, and low *in vitro* and *in vivo* clearances suitable for further development.

The discovery of compound **22** paved the way for the development of nirmatrelvir **2** as the first SARS-CoV-2 3CLpro inhibitor drug for the treatment of COVID-19. Rat oral bioavailability of compound **22** was limited (F=1.4%). To improve oral absorption, other warheads were designed to reduce the hydrogen bonding ability of the α-hydroxymethyl ketone warhead in **22**. Introduction of nitrile functionality resulted in compound **23** with good enzyme activity, and an improvement in oral bioavailability (F=7.8%), however, antiviral activity was reduced compared to **22**. Incorporation of a boceprevir P2 ligand, 6,6-dimethyl-3-azabicyclo[3.1.0] hexane in place of P2 leucine and

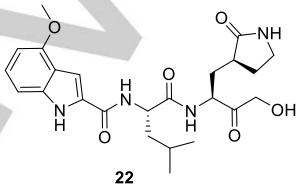

22
IC_{50} = 0.27 nM
EC_{50} = 231 nM (VeroE6)

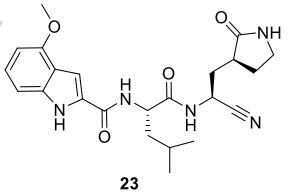

23
IC_{50} = 27.7 nM
EC_{50} = 1364 nM (VeroE6)

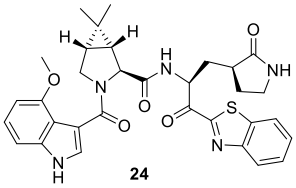

24
IC_{50} = 230 nM
EC_{50} = 5593 nM

Figure 15. SARS-CoV-2 3CLpro Inhibitor **22-24**

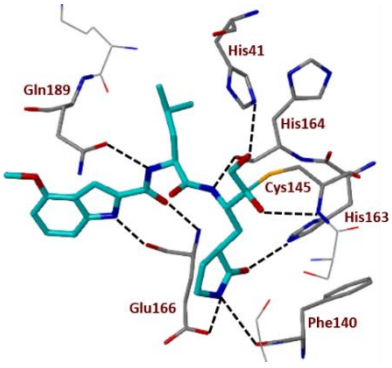

Figure 16. X-ray structure of **22**-bound 3CLpro

benzothiazol-2-yl ketone as the warhead resulted in compound **24**, which showed reduction of both enzyme and antiviral activity.

Replacement of the methoxyindole P3 ligand with a (*S*)-val-sulfonamide derivative resulted in compound **25** (Figure 17) with improved activity and slight improvement in oral bioavailability (F=10%). Inhibitor **26** resulted from varying the sulfonamide P3-capping group with a trifluoroacetamide group. This compound exhibited comparable enzymatic inhibitory activity to **25**; however, its antiviral activity in VeroE6 cells improved nearly 10-fold. Furthermore, this replacement resulted in a significant improvement in the oral bioavailability in rats (10 mpk, F=33%). Introduction of a P1' nitrile and replacement of the (*S*)-val with a (*S*)-*tert*-leucine provided compound **2** with further improvement in activity as well as oral bioavailability in rats (10 mpk, F=50%). This compound became known as PF-07321332 (**2**). It exhibited low oral bioavailability in monkeys (10 mpk, F=8.5%) due to first-pass metabolism along the gastrointestinal tract by cytochrome P450 (CYP) enzymes. Subsequent experiments involving co-administration with CYP34A inactivator, ritonavir (RTU) significantly improved the plasma concentration of PF-07321332.[47]

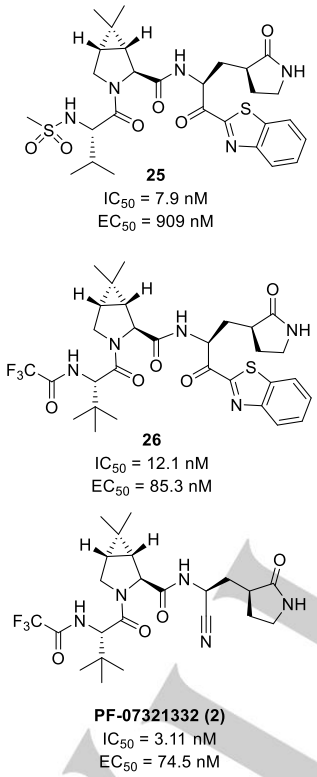

Figure 17. Development of nirmatrelvir **2** (PF-07321332)

The X-ray co-crystal structure of inhibitor **2** with SARS-CoV-2 3CLpro was determined. As shown in Figure 18, the P1' nitrile functionality of compound **2** forms a reversible covalent thioimidate adduct with the catalytic Cys145. The P1 lactam carbonyl forms a hydrogen bond with His163 and the lactam NH forms a hydrogen bond with the side chain carboxylic acid of Glu166 similar to other structures. A recent report by Kovalevsky and co-workers extensively explored the active site interactions of three in house compounds and inhibitor **2**.[81] Interestingly, it was reported that the active site of Mpro can, and does, undergo a significant amount of distortion to accommodate bulkier substituents, particularly in the S4 and S5 subsites. Nitrile warhead compounds, including **2**, were examined utilizing room temperature X-ray crystallography. Results displayed the presence of the thioimidate adduct formation with Cys145 and subsequent N insertion into the oxyanion hole. Other important interactions are the unconventional interactions with the CF_3 group. The small electronegative CF_3 is capable of forming favorable F…O interactions, as shown in this study, or F…N interactions, as reported in another study[82], with the protease. These types of unconventional interactions have shown to be of significant importance in inhibitor activity, metabolic stability, and pharmacokinetics.

This oral SARS-CoV-2 3CLpro inhibitor (Figure 17, inhibitor **2**) and its entrance into clinical trials were unveiled by Pfizer in April 2021.[83] As such, it is the first orally administered compound to enter clinical trials that targets the main protease of SARS-CoV-2. It can be taken orally as a pill or capsule, allowing for the freedom to be given outside of hospitals.

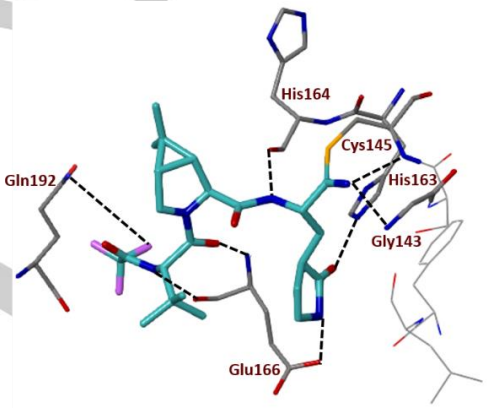

Figure 18. PF-07321332 bound 3CLpro (PDB 7VH8)

Interestingly, the first 7 mg of the compound were synthesized in late July 2020.[83] A massive scale up effort was undertaken and by late October 100 g of the compound was synthesized, and two weeks later the chemists were able to scale up the synthesis to even more than 1 kg.[83]

According to phase II and III clinical trial data, inhibitor **2** or nirmatrelvir, is extremely effective in reducing the risk of COVID-19 related hospitalization and death. Nirmatrelvir is marketed and sold under the name paxlovid, which is a combination of nirmatrelvir and ritonavir. As nirmatrelvir is metabolized by CYP3A4, ritonavir is necessary as a pharmacokinetic booster to increase the oral bioavailability of nirmatrelvir.[84] In a randomized clinical trial with 1:1 paxlovid:placebo received orally every 12 hours for five days, it was found that those receiving paxlovid had significantly reduced hospital admissions and deaths among those affected by COVID-19.[85] It was found that among participants who received treatment within three days of beginning COVID-19 symptoms, the risk of hospitalization or death was 89% lower than that for the placebo group.[85,86] Phase II/III clinical trials for administration of paxlovid in pediatric patients between the ages of 6 and 12 who test positive for COVID-19 and are at risk for severe disease began in March of 2022.[87]

A recent report by Pfizer researchers and collaborators reports the activity of nirmatrelvir against several SARS-CoV-2 variants of concern and variants of interest.[88] Nirmatrelvir results are compared to the FDA approved remdesivir as the control.

Table 1: Pfizer nirmatrelvir variant antiviral activity studies

Variant	Drug	EC_{50} (nM)
USA-WA1	Remdesivir	15.4
	Nirmatrelvir	32.2
α	Remdesivir	7.0
	Nirmatrelvir	41.0
β	Remdesivir	14.8
	Nirmatrelvir	127.2
γ	Remdesivir	3.9
	Nirmatrelvir	24.9
λ	Remdesivir	3.3
	Nirmatrelvir	21.2
δ	Remdesivir	1.9
	Nirmatrelvir	15.9
μ	Remdesivir	5.8
	Nirmatrelvir	25.7
o	Remdesivir	3.2
	Nirmatrelvir	16.2

Results in Table 1 indicate that nirmatrelvir does in fact potently inhibit the many variants. EUA was granted to Pfizer for paxlovid on December 22, 2021 for the treatment of mild-to-moderate COVID-19 in adults and pediatric patients 12 years of age or older weighing at least 40 kg who have tested positive for COVID-19 and who are at high risk for progression to severe disease including hospitalization or death. A recent study by Pan and co-workers reported the treatment of omicron infected calu-3 cells with varying doses of nirmatrelvir and observed potent inhibition of viral RNA.[86] Calculated IC_{50} values against the wild type variant and omicron variant were reportedly 0.176 μM and 0.0246 μM, respectively.[86]

4.1.2 Small Molecule Covalent SARS-CoV-2 3CLpro Inhibitors

Indole-5-chloropyridinyl esters were designed and synthesized to inhibit SARS-CoV-1 3CLpro.[61,89] Several derivatives have been shown to potently inhibit the 3CLpro enzyme by formation of a covalent bond with the catalytic Cys145 residue in the active site. Ghosh and co-workers further investigated the potential of this class of compounds as SARS-CoV-2 3CLpro inhibitors with the outbreak of COVID-19.[89,90] A number of compounds with varying substituents and functionalities have been synthesized and evaluated. Structure-activity studies show that the position of the carboxylic acid on the indole ring is important for activity. Selected representative derivatives **27-31** are shown in Figure 19. Among them, inhibitor **27** displayed a SARS-CoV-2 3CLpro inhibitory IC_{50} value of 250 nM. The compound also exhibited potent antiviral activity with an EC_{50} value of 2.8 µM in VeroE6 cells. Remdesivir, an RdRp inhibitor, showed an antiviral EC_{50} value of 1.2 µM in the same assay. Furthermore, compound **27** and remdesivir exhibited comparable antiviral activity in immunocytochemistry assays.[61]

The X-ray structures of compound **27**-bound to SARS-CoV 3CLpro and SARS-CoV-2 3CLpro were determined. Both structures revealed that catalytic Cys145 formed a covalent bond with the indole ester carbonyl group of compound **27**. The X-ray crystal structure of **27**-bound to SARS-CoV-2 3CLpro is shown in Figure 20. Interestingly, the indole ring forms π-π stacking interactions with the imidazole ring of the His41.

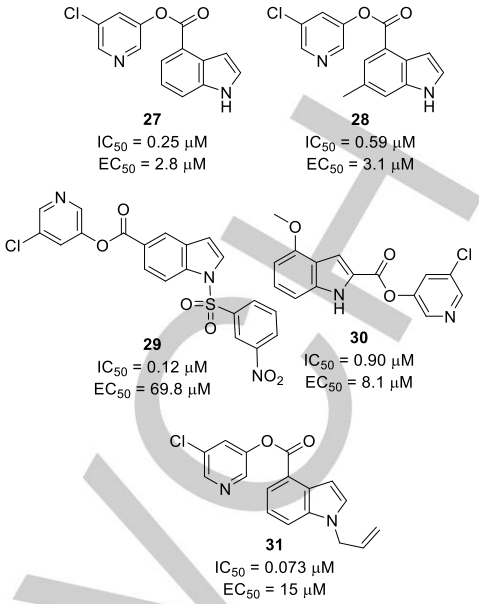

Figure 19. 5-chloropyridinyl ester SARS-CoV-2 covalent inhibitors

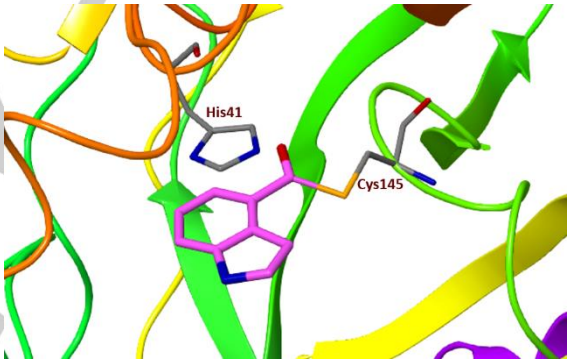

Figure 20. Indole chloropyridinyl ester **27** (magenta) bound SARS-CoV-2 3CLpro (PDB 7RBZ).

Methyl substitution on the indole ring was also investigated to lock the bioactive conformation of the pyridyl ester. Incorporation of the methyl at position 3 resulted in significantly reduced enzyme and antiviral activity. However, incorporation of the methyl at position 6 resulted in compound **28**. This compound exhibited comparable 3CLpro inhibitory and antiviral activity to compound **27**. An inhibitor with the methyl at the 5 position of the indole displayed no antiviral activity. Varying the position of the chloropyridinyl ring to the 2 or 5 position of the indole led to a reduction in activity (compounds **29** and **30**) compared to **27**. The original study displayed this loss directly for the 5-indole chloropyridinyl ester, but inhibitor **29** was noted to be even less potent. This further loss of activity may be attributed to the large sulfonamide, which could cause unfavorable steric interactions in the active site. Substitution of the chloropyridinyl ester at the 4 position of the indole ring also showed a reduction in enzyme inhibition and a decrease in antiviral activity.

Substitutions on the indole ring and the chloropyridine ring were also examined. Addition of a 3-nitro sulfonamide on the

indole nitrogen led to compound **29**, which showed improved enzyme inhibitory activity but a decrease in antiviral activity

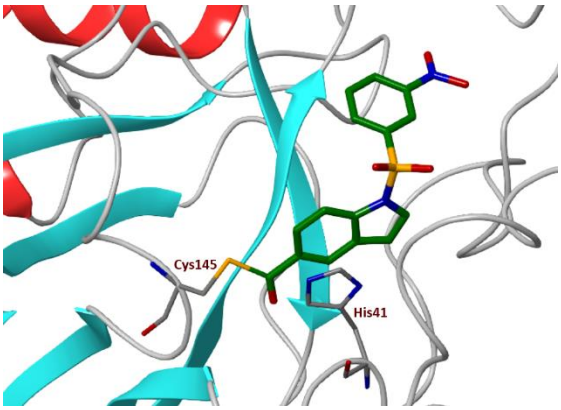

Figure 21. Inhibitor **29** (green) bound SARS-CoV- 3CLpro (PDB 7RC1).

compared to **27**. However, addition of an *N*-allyl substituent at this position led to potent derivative **31** with a 3CLpro inhibitory IC_{50} of 73 nM. Although, antiviral EC_{50} was reduced to 15 μM. An X-ray crystal structure of sulfonamide **29** bound to SARS-CoV-2 3CLpro was determined and the structure is shown in Figure 21. Confirmation of the covalent nature can be observed in the thioester formation between Cys145 and the carbonyl of the inhibitor. Another important interaction is shown in the π-π stacking of the inhibitor indole ring with the imidazole ring of His41.[89] Subsequent studies in other laboratories have expanded upon these studies utilizing compound **27** as a lead. Pillaiyar and co-workers investigated a series of small molecule thioesters, and Müller's group used an in house protocol to identify lead compounds and performed a small subsequent optimization study.[91,92]

The design and synthesis of a series of 5-chloropyridinyl esters of common nonsteroidal anti-inflammatory agents (NSAID) has been investigated by Ghosh and co-workers.[90] The chloropyridinyl esters of salicylic acid, ibuprofen, indomethacin, and related aromatic carboxylic acids exhibited potent moderate nanomolar enzyme inhibitory activity. As highlighted in Figure 22, acetoxysalicylic acid derivative (aspirin-derived) **32** showed SARS-CoV-2 3CLpro inhibitory activity of 360 nM. Antiviral activity was determined using a quantitative VeroE6 cell-based assay with RNA-qPCR as described recently.[61,93] However, these compounds did not show appreciable antiviral activity. Salicylic acid and methyl substituted derivatives were prepared and evaluated. Methyl group substitution on the aromatic ring resulted in the synthesis of monomeric, dimeric, and trimeric ester derivatives. Monomeric derivatives **33-35** showed moderate nanomolar 3CLpro inhibitory activity; however, only the 5-methyl derivative **35** showed antiviral activity (EC_{50} value 46 µM). Representative dimeric compound **36** showed slightly higher 3CLpro inhibitory activity. These compounds did not show cytotoxicity up to 100 µM.

Racemic ibuprofen derivative **37** showed moderate enzyme inhibition and essentially no antiviral activity. (*R*)-Naproxen-derived ester **38** exhibited significantly better 3CLpro inhibitory activity (IC_{50} of 160 nM) over (*S*)-naproxen-derived **39**. However, both compounds did not show much antiviral activity. The mode of inhibition presumably involves the formation of a covalent bond with catalytic Cys145 and the ester carbonyl carbon in the active site. An active model of more potent (*R*)-naproxen derivative **38**-bound 3CL protease has been presented. The model in Figure 23 shows formation of a covalent bond with

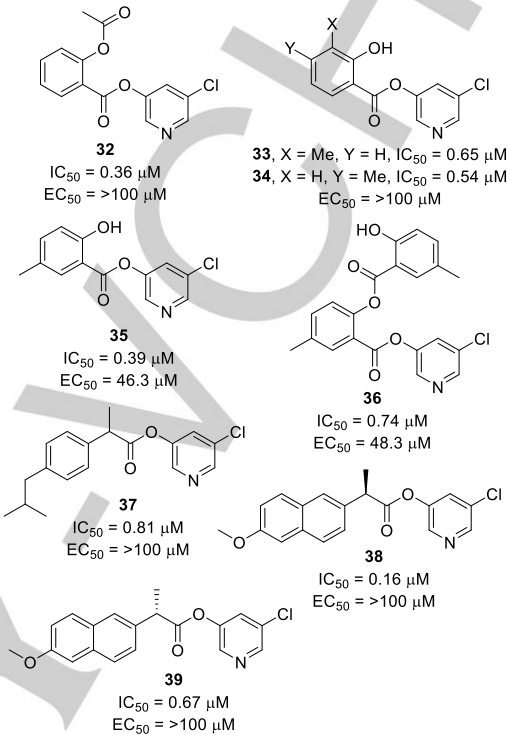

Figure 22. NSAID derived SARS-CoV-2 3CLpro inhibitors.

Cys145 and a strong hydrogen bond with Gln189. Also, His41 forms a nice π-π stacking interaction with the napthyl ring of (*R*)-naproxen and similar π-π stacking interactions to those observed in other X-ray crystallographic studies of indole-derived active ester derivatives as shown above.

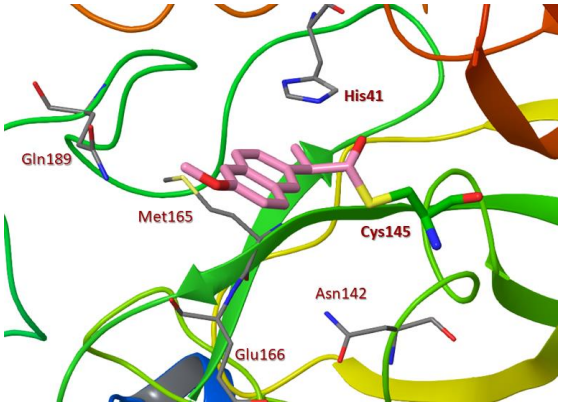

Figure 23. An active site model of inhibitor **38** (violet) with SARS-CoV-2 3CLprotease. (PDB 7RBZ).

Zhang and collaborators reported a series of SARS-CoV-2 3CLpro inhibitors that incorporated pyrogallol warheads.[94] Initial screening of flavonoid natural products led to the discovery that myricetin **40** and dihydromyricetin **41**, shown in Figure 24, exhibited potent 3CLpro inhibitory activity (>90% inhibition).[94] The

X-ray structure of myricetin-bound SARS-CoV-2 3CLpro was determined. As depicted in Figure 25, structural analysis revealed that myricetin forms a covalent bond with Cys145.

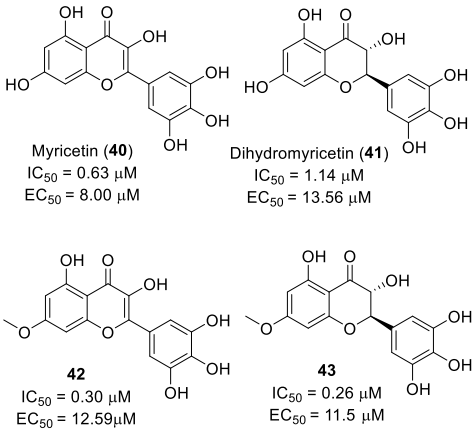

Figure 24. Pyrogallol 3CLpro Inhibitors **40-43.**

Based on these results, investigators synthesized several other derivatives by O-alkylation of 7-OH group. Introduction of methyl, ethyl, isoamyl, and cyclopentylmethyl groups were examined to make interactions in the sub-pocket of 3CLpro. It turned out that the methyl ether derivatives improved 3CLpro activity of myricetin and dihydromyricetin derivatives **42** and **43**. Interestingly, other larger alkyl groups decreased potency. The dihydromyricetin derivative **43** was found to have good activity. PK profiling of **43** showed 18% oral bioavailability in rats and a favorable plasma duration of 1.89 h, which indicated the possibility of further development as an oral drug.

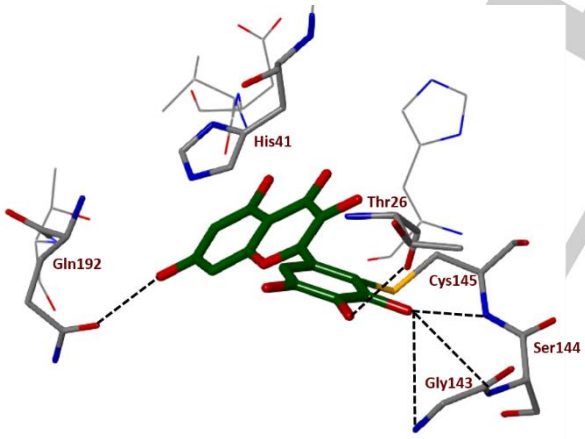

Figure 25. Myricetin **40** (green) bound SARS-CoV-2 3CLpro (P DB 7DPP)

Yarovaya and co-workers reported the design, synthesis, and evaluation of a series of bispidine based SARS-CoV-2 3CLpro inhibitors.[95] All derivatives were examined against SARS-CoV-2 3CLpro. Many compounds were found to have inhibitory activity ranging from 1-10 μ M, and several compounds exhibited submicromolar activity. Unsubstituted bispidinone, **44** in Figure 26, exhibited an IC_{50} of 2.6 μM. Other substituted bispidine derivatives, including amide derivatives **45** and derivatives without a carbonyl at C9 (**46**) were prepared and evaluated. In general, amide derivatives **45a-c** were active; however, derivatives **46** without the C-9 ketone carbonyl were mostly inactive. *Bis*-amide derivatives **45a** and **45b** in Figure 27 displayed a 3CLpro IC_{50} value of 1.4 μM. Inhibitor **45c,** containing the dihydrobenzo indazole, exhibited the best activity. Also, *N*-alkyl derivatives **47a** and **47b** displayed low micromolar inhibitory activity. In general, compounds with the scaffold of inhibitors **47** showed promising results with many of them in the low micromolar range. All compounds were also tested for their cytotoxicity in HEK293T cells and were found to be nontoxic.

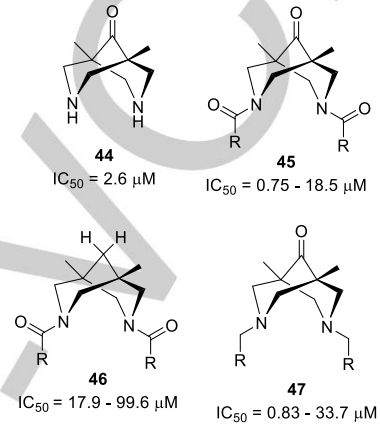

Figure 26. *Bis*-pidinone-derived 3CLpro inhibitors **44-47.**

The mechanism of action was speculated to involve the formation of a covalent bond with Cys145 via the carbonyl at C9.[95] ADMET analysis was performed on these compounds, and of those that displayed good drug-like properties. Compound **47a** also displayed good in vitro activity.[95]

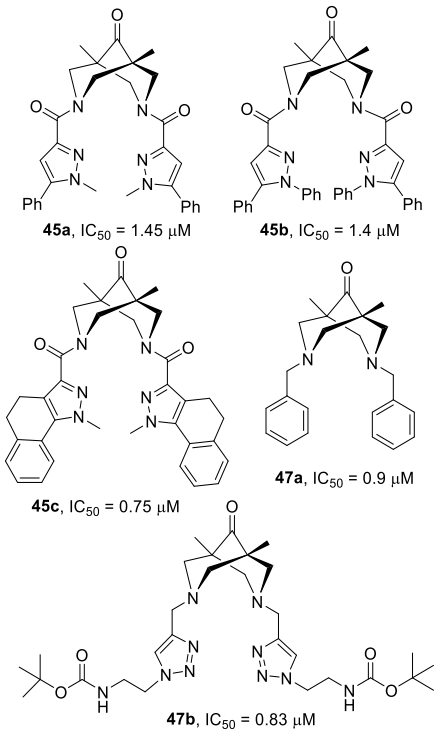

Figure 27. Potent bispidinone-derived inhibitors **45a-c** and **46a-b.**

4.1.3 Noncovalent Reversible Inhibitors

In 2013, Jacobs and co-workers discovered a novel class of non-covalent SARS-CoV-1 3CLpro inhibitors following a screening of NIH molecular libraries. As shown in Figure 28, an initial hit provided lead compound **48** as an inhibitor of both SARS-CoV-1 3CLpro and PLpro enzymes.[96] Subsequent synthesis of derivatives and SAR exploration led to the identification of active racemic compound **49** and the stereochemically defined, more active isomer **50**. This *R*-isomer showed a 3CLpro IC_{50} value of 1.5 μM, and it is more potent than the S-isomer (IC_{50} 28 μM). The X-ray structure of compound **50**-bound SARS-CoV-1 3CLpro was determined and the structure provided detailed molecular interactions in the SARS-CoV-1 3CLpro active site. Detailed structural analysis revealed that compound **49** inhibits 3CLpro enzyme without forming a covalent bond with catalytic Cys145. Compound **50** fills in the S3-S1' subpockets of SARS-CoV-1 3CLpro. This discovery triggered further search of potent compounds through the synthesis of novel derivatives and this has been reviewed recently. With the outbreak of SARS-CoV-2, many laboratories further explored the potential of these lead structures by synthesizing other structural variants.

Kitamura and collaborators examined a series of derivatives as potential SARS-CoV-2 3CLpro inhibitors.[97] Representative compounds **51-53** in Figure 29 showed SARS-CoV-2 3CLpro inhibitory activity, with inhibitors **51** and **52** showing submicromolar activity. Compound **51** showed a SARS-CoV-2 3CLpro K_i value of 0.2 μM. It was tested against SARS-CoV-2 in VeroE6 cells using the immunofluorescence assay, and it was found to have an EC_{50} of 1.27 μM.[97] This compound did not show any activity against SARS-CoV-2 PLpro. Also, compound **51** did not exhibit any cytotoxicity against VeroE6 cells up to 100 μM.[97] Compound **52** with a biphenyl group as the P2 ligand, benzylmethyl as the P3 ligand, and imidazole as the P1' ligand

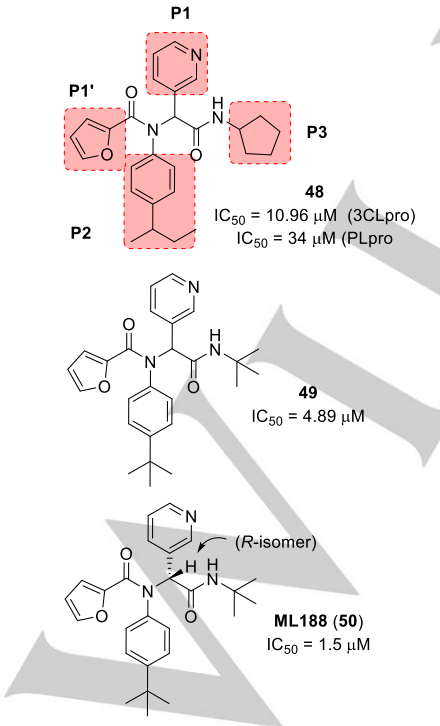

Figure 28. Noncovalent SARS-CoV-2 3CLpro Inhibitors

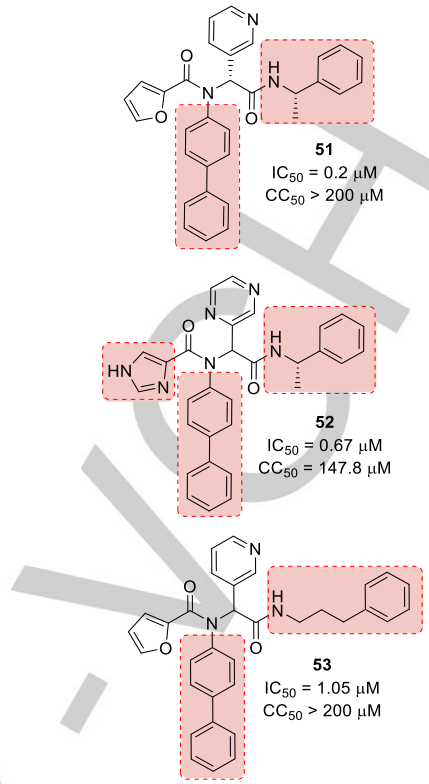

Figure 29. Noncovalent Inhibitors **51–53.**

showed a 3CLpro inhibitory activity of 0.67 μM. In general it was found that the biphenyl P2 ligand and the benzyl methyl P3 were the most active substitutions. An X-ray crystal structure of **51** bound to SARS-CoV-2 3CLpro was determined. As shown in Figure 30, there is no covalent interaction with Cys145, as was previously shown with the **50**-bound SARS-CoV-1 3CLpro structure.

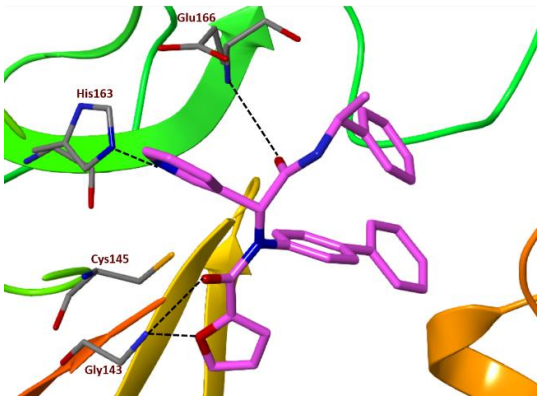

Figure 30. Noncovalent Inhibitor **51** (magenta) bound 3CLpro (PDB 7KX5).

Ma and co-workers have reported the synthesis of Ugi-derivatives with a P1'- dichloroacetamide, dibromoacetamide, tribromoacetamide, 2-bromo-2,2-dichloroacetamide, and 2-chloro-2,2-dibromoacetamide functionalities.[98] As highlighted in Figure 31, compounds **54** and **55** were found to be the most potent with SARS-CoV-2 3CLpro IC_{50} values of 0.43 μM and 0.08

μM, respectively. Compound **55** showed antiviral activity in VeroE6 and Caco2-hACE2 cells with EC_{50} values in the low micromolar range. The compound also displayed good selectivity (greater than 20 μM) against calpain I, cathepsin B, cathepsin K, caspase-3 and trypsin.[98] Structural analysis showed that the chloroacetamide or bromoacetamide warheads form a covalent linkage with Cys145 and the rest of the molecule interacts similar to other noncovalent inhibitors described previously.

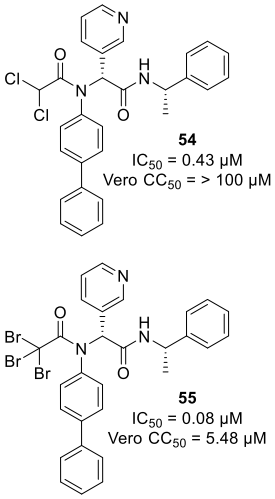

Figure 31. Dichloroacetamide and tribromoacetamide 3CLpro Inhibitors

Jorgensen and collaborators reported an interesting series of potent noncovalent and nonpeptidic inhibitors.[99] The investigators carried out virtual screenings of 2,000 known, approved drugs, and found 14 hits as inhibitors of SARS-CoV-2 3CLpro.[99] As shown in Figure 32, perampanel (**56**) was chosen as a lead compound. Further design and optimization based upon docking studies of compound **56** with 3CLpro were carried out. As highlighted, several potent derivatives, such as **57-59**, were identified. Propoxy derivative **57** showed an enzyme IC_{50} value of 140 nM and an antiviral activity of 2.5 µM. Benzyloxy derivative **58** also showed potent 3CLpro inhibitory activity with an IC_{50} value of 128 nM. Compound **59** exhibited the most potent activity with an IC_{50} value of 18 nM. However, this compound did not show antiviral activity.

A crystal structure with synthesized derivative **57** with 3CLpro was determined. As shown in Figure 33, catalytic Cys145 does not make any covalent bond with the inhibitor. The side pyridine nitrogen forms a hydrogen bond with His163 in the active site. The pyridine carbonyl group forms a hydrogen bond with the backbone NH of Glu166. A hydrogen bonding interaction between the nitrile and amide nitrogen of Gly143 can also be observed. Further structural modifications are highlighted in Figure 34. Monofluoro derivative **60** was also found to be very potent. Overall results showed that this series of inhibitors are quite potent and show promise for further development. Inhibitors **61** and **62** also exhibited good activity. Inhibitor **59** shows synergistic effects with the FDA approved polymerase inhibitor remdesivir.[99] Inhibitor **62** turned out to be the most potent with an EC_{50} value of 1.1 μM.

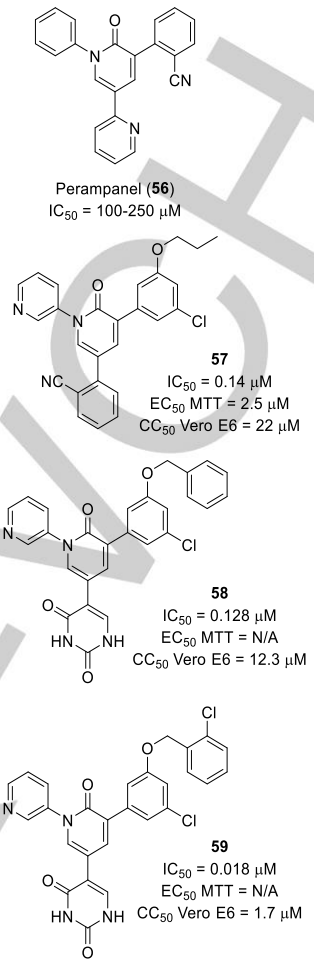

Figure 32. Noncovalent Perampanel Derived Inhibitors **56-59.**

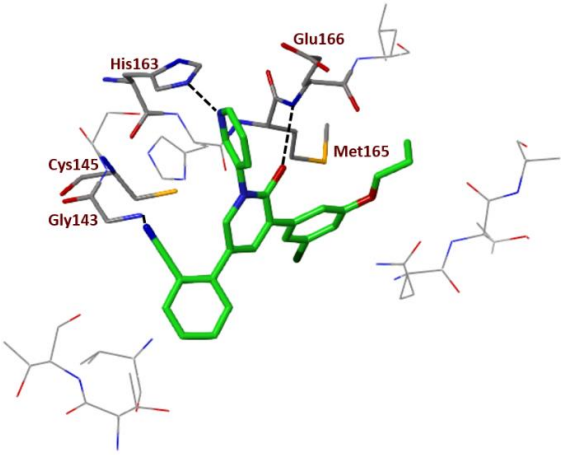

Figure 33. Inhibitor **57** (green) bound 3CLpro (PDB 7L11)

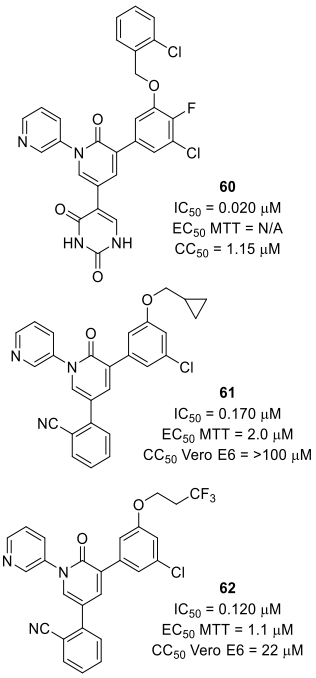

Figure 34. Perampanel Derived Inhibitors **60-62.**

Stauffer and collaborators reported a series of noncovalent SARS-CoV-2 3CLpro inhibitors.[100] Lead compound ML300 (**63**) was a MLPCN probe compound that was chosen for optimization studies. ML300 was initially developed in the wake of the SARS-CoV-1 outbreak, and was chosen as the lead compound based on several factors including the need for further optimization to improve ADME properties like metabolic stability.[96] A crystal structure with **63** (Figure 35) bound SARS-CoV-2 3CLpro was obtained depicting key interactions in the enzyme-inhibitor complex shown in Figure 36. Several key hydrogen bonding interactions are observed. The benzotriazole nitrogen forms a hydrogen bond with the side chain of His163. The amide carbonyl of **63** forms a hydrogen bonding interaction with the backbone nitrogen of Glu166, and the terminal amide associated with the cyclopropane forms a hydrogen bond with the alcohol of Ser46. The benzotriazole and Cys145 are involved in an interesting interaction with a slightly longer hydrogen bond.[100]

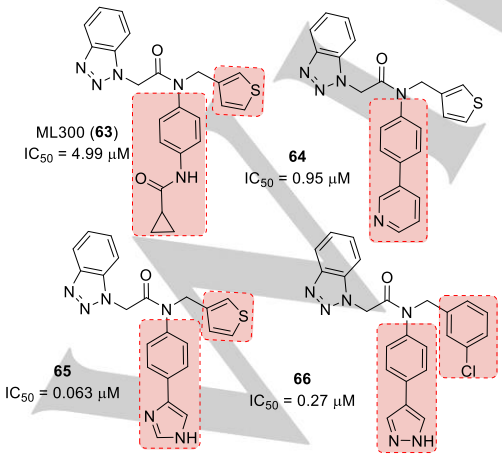

Figure 35. Noncovalent 3CLpro Inhibitors **63-66**

Lead optimization efforts of ML300 originally led to inhibitor **64** with an IC_{50} of 0.95 μM against SARS-CoV-2 3CLpro, which was comparable to that of SARS-CoV-1 3CLpro. Several sub sites were varied, as shown in the lead compound. Imidazole derivative **65** exhibited very good nanomolar potency. N-methylated derivatives of either pyrazole or imidazole inhibitors lost considerable potency, likely due to the loss of a hydrogen bond donor. The replacement of the thiophene moiety on **65** with a 3-chlorophenyl group resulted compound **66**, exhibiting an IC_{50} of 0.27 μM.

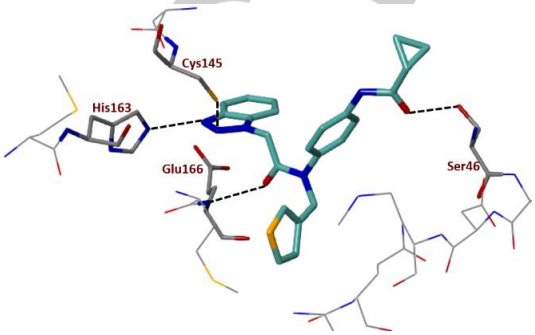

Figure 36. Inhibitor **63** bound 3CLpro PDB 7LME

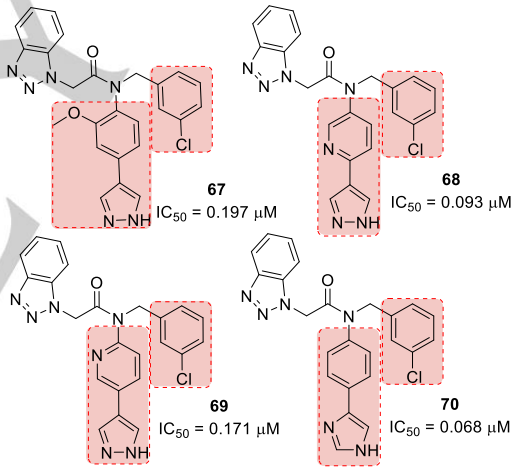

Figure 37. Noncovalent Inhibitors **67 – 70.**

Further optimization keeping the benzotriazole and the 3-chlorophenyl as fixed ligands led to potent compounds **67-70** shown in Figure 37. Antiviral activities of the most promising compounds were tested in VeroE6 cells using the cytopathic effect inhibition and in a plaque reduction assay.[100] Lead compound ML300 showed an EC_{50} of 19.9 μM in the live virus cytopathic effect (CPE) assay, whereas derivative **66** had an improved EC_{50} value of 1.7 μM in the CPE assay. It was observed that derivatives that substituted the thienyl moiety for 3-chlorophenyl displayed much better antiviral activity. Compound **70** displayed submicromolar activity in both assays and had a good selectivity index.

Unoh and co-workers reported a novel series of noncovalent SARS-CoV-2 3CLpro inhibitors, one of which is

undergoing clinical trials in Japan.[101,102] A structure-based virtual screening was utilized to identify lead compounds from their in-house compound library. One of the lead compounds, **71** (Figure 38), showed a SARS-CoV-2 3CLpro IC_{50} value of 8.6 μM.[101] The X-ray structure of compound **71**-bound SARS-CoV-2 3CLpro was determined. Subsequent structure-based optimization led to potent derivatives, one of these potent compounds was **72** (S-217622), which was selected for clinical development.

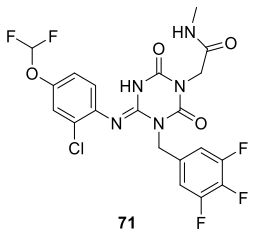

71
IC_{50} = 8.6 μM
EC_{50} = Not Tested

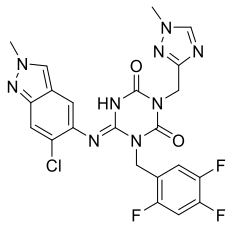

72 (S-217622)
IC_{50} = 0.013 μM
EC_{50} = 0.29 - 0.5 μM

Figure 38. SARS-CoV-2 3CLpro noncovalent inhibitors **71 and 72**

Inhibitor **72** exhibited potent in vitro activity against all tested SARS-CoV-2 variants including α, β, γ, δ, and o strains. Inhibitor **72** also showed no inhibition of host cell proteases including caspase-2, chymotrypsin, cathepsin B, cathepsin D, cathepsin G, cathepsin L and thrombin.[101] In vivo efficacy was also tested with SARS-CoV-2 infected mice, yielding favorable results. Treatment groups displayed considerably lower viral loads than non-treatment groups.[101] These favorable results have allowed this orally active drug to progress to clinical trials in Japan, where it has completed Phase IIa.[102] The efficacy and safety of a once daily dose over 5 days were evaluated, and showed a decrease in viral loads of 60-80% compared to the placebo group.[102] Since then, approval for manufacture and sales in Japan were filed and an NIH funded global Phase III clinical trial has been announced. This clinical candidate does not require co-administration of another drug and can be given once daily.[102]

The X-ray co-crystal structure of **72**-bound 3CLpro was determined. As shown in Figure 39, the 1-methyl-1H-1,24-triazole moiety occupies the S1 pocket and forms a hydrogen bond with the side chain NH of His163. The 2,4,5 trifluorobenzyl group fits in the S2 site and is involved in π-π stacking interactions with the imidazole side chain of His41. The P1' ligand 6-chloro-2-methyl-2H-indazole forms a hydrogen bond with the backbone NH of Thr26. It also shows hydrophobic contacts with Met49.

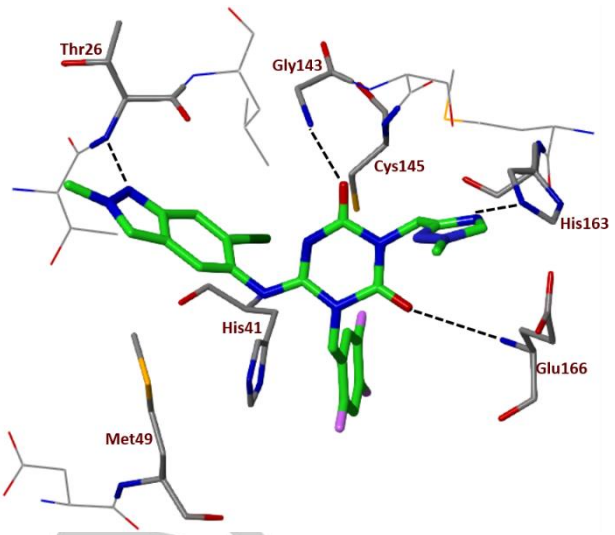

Figure 39. Inhibitor **72**-bound 3CLpro (PDB code: 7VU6).

4.2 PLpro Inhibitors

SARS-CoV-2 PLpro is also an important drug design target since it plays a critical role in the coronavirus replication cycle.[10,103] In particular, PLpro is involved in processing and maturation of viral polyproteins, assembly of the replicase-transcriptase complex, and disruption of host immune response.[104,105] The X-ray crystallographic studies of SARS-CoV-1 PLpro, noncovalent inhibitor design, and a number of inhibitor-bound SARS-CoV-1 PLpro were previously reported and reviewed.[9,106,107] Recently, X-ray structural studies of GRL-0617-bound SARS-CoV-2 PLpro have been reported.[108,109,110] Osipiuk and co-workers reported a high resolution X-ray structure of inhibitor **73** (GRL-0617)-bound SARS-CoV-2 PLpro.[108] As can be seen in the co-crystal structure in Figure 40, the benzamide moiety forms hydrogen-bonding interactions with the main chain nitrogen of Gln270 and side chain of Asp165. Replacing this moiety with a benzylamine or benzyl sulfonamide isostere led to a significant reduction in potency and this portion was conserved in subsequent optimization studies.[108,111] Subsequently, they designed a number of inhibitors (**74**-**76**) highlighted in Figure 41.

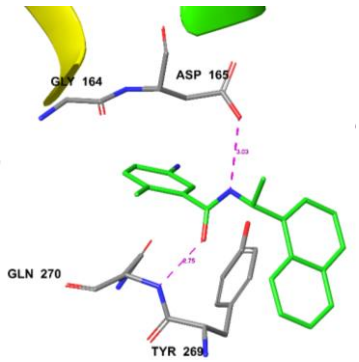

Figure 40. Inhibitor **73**-bound PLpro PDB 3E9S

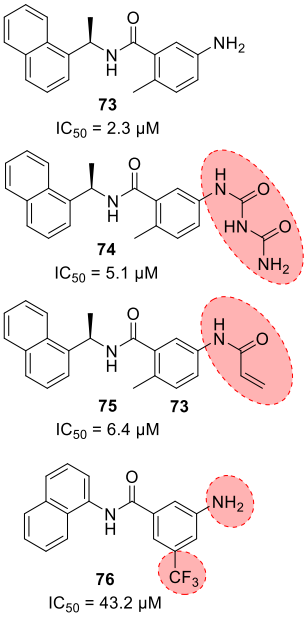

Figure 41. PLpro Inhibitors **74-76.**

All compounds have shown comparable SARS-CoV-2 PLpro activity and a few of them displayed antiviral acitivity, but are less potent than compound **73**. An investigation by Shan et al. expanded upon the naphthyl derivatives.[112] Two of their most potent compounds were found to have low micromolar activity in their novel assay.

Shen and co-workers reported a series of SARS-CoV-2 PLpro inhibitors via high-throughput screening.[111] They utilized the naphthalenyl benzamide core structure of **73** as reported previously.[106] As highlighted in Figure 42, naphthalenyl derivative **77** is less potent than inhibitor **73,** and as such it was noted that any variation in the benzylmethyl led to a loss in activity.

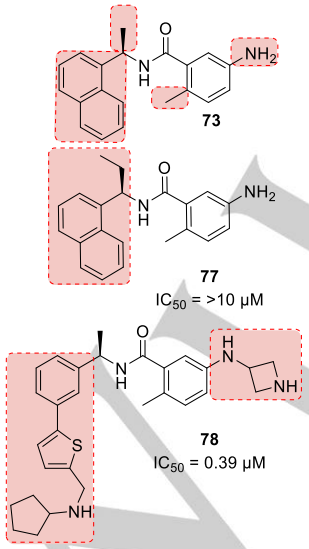

Figure 42. PLpro Inhibitors **77** and **78.**

Replacement of the naphthalene of **77** was then investigated. This was done in an attempt to improve metabolic stability. Fused heteroaryls such as benzothiophene, indole, and carbazole with differing linkages were investigated. Unfortunately, most modifications led to a loss in activity. The 3- benzothiphene and carabazole based analogues had reasonable potency. The biaryl derivatives such as 2-phenylthiphene and 3-phenylthiophene, however, showed a slight improvement in potency in compound **78**.

Further modifications are shown in Figure 43. Modification of the aryl amine to an azetidine ring resulted in a dramatic increase in potency due to enabling the electrostatic interactions with Glu167. Two of their most potent inhibitors, **78** and **79**, were tested for their efficacy and bioavailability in human lung epithelial A549 cells. Inhibitor **81** was not effective in preliminary antiviral studies compared to the other two inhibitors, although it had a high binding affinity and low dissociation rate. Both **78** and **79** displayed more cytotoxicity than **77** at 100 μM and no cytotoxicity up to 30 μM.

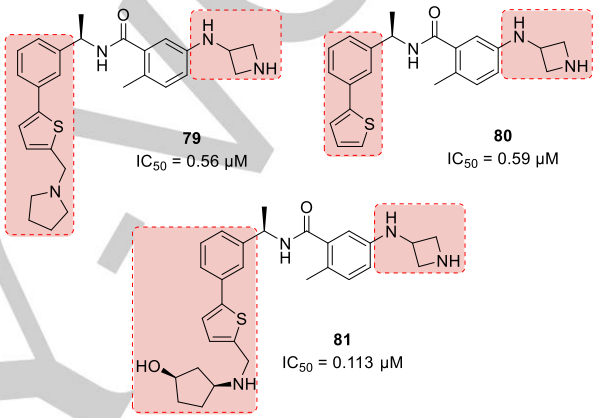

Figure 43. PLpro Inhibitors **72 – 74.**

5. RdRp Polymerase Inhibitors

RdRp is a nonstructural protein responsible for synthesizing viral RNA, which is then transcribed into viral proteins. Inhibition of this essential enzyme prevents protein synthesis, a vital step in the viral life cycle. This is also the only protein that is mostly conserved among RNA viruses, making it an attractive target for broad-spectrum antivirals.[113]

5.1 RdRp Nucleoside Inhibitors

Nucleoside inhibitors mimic substrates for the viral RdRp and lead to either chain termination or lethal mutagenesis. Unfortunately, nucleoside derivatives, particularly those that cause chain termination, can be less effective against coronaviruses. Coronaviruses contain an exonucleolytic proofreading mechanism that can remove misincorporated nucleotides.[114] Therefore, these drug therapies need to be effective at circumventing the natural proofreading ability of RdRp. Remdesivir (**1**, Figures 2 and 44) is an antiviral nucleotide phosphoramidate prodrug initially developed for treatment of Hepatitis C and later utilized as a therapy for Ebola and Marburg viral infections.[115] Remdesivir triphosphate is the active form of the drug and a natural drug metabolite that competes with the native adenosine triphosphate for chain inclusion.[115,116] Inclusion of remdesivir into the RNA chain prevents further RNA synthesis and leads to chain termination. This termination has been shown

to be the result of a translocation barrier, which causes the coronavirus RdRp to stall after the addition of three nucleotides after incorporation of remdesivir.[117,118] This is expected to occur due to the C1 nitrile in remdesivir, as it has been shown to be crucial for antiviral potency in the Ebola virus.[117] Molecular modeling has also shown a steric clash between the nitrile of remdesivir and side chain of Ser861 in the Nsp12 subunit of RdRp.[117] To combat this, viral proofreading can occur, which renders remdesivir less efficient. Figure 45 illustrates remdesivir and SARS-CoV-2-RdRp active site interactions based upon X-ray structural studies.[118]

Several studies have been done to show remdesivir efficacy; however mixed results have been observed. Clinical trials with remdesivir have been performed to determine its effect on patients with moderate COVID-19 versus standard of care, as well as the effect of a 5 day remdesivir treatment compared to 10 day treatment regimen.[119,120] In the randomized, open-labeled trial of hospitalized patients with confirmed COVID-19 pneumonia across 105 hospitals in the US, Europe, and Asia it was found that these patients with moderate COVID-19 no statistical significance was observed for those that were treated with remdesivir for 10 days. However, a statistically significant difference was observed for those that received a 5-day treatment of remdesivir compared to standard of care treatment. This difference was of uncertain clinical importance though.[119] In another randomized, open-label phase III clinical trial involving hospitalized patients with confirmed severe COVID-19 it was found that there was no significant difference between a 5-day and 10-day treatment regimen of remdesivir. A large, double-blind, randomized, placebo-controlled clinical trial of remdesivir treatment of COVID-19 was published on November 5, 2020.[36] This was one of the larger studies and included patients of varying levels of COVID-19 infection. It was observed that those that received treatment with remdesivir had a median recovery time of 10 days as opposed to 15 days in the placebo control group.[36] Patients who received remdesivir were also found to be more likely than those who received a placebo to have clinical

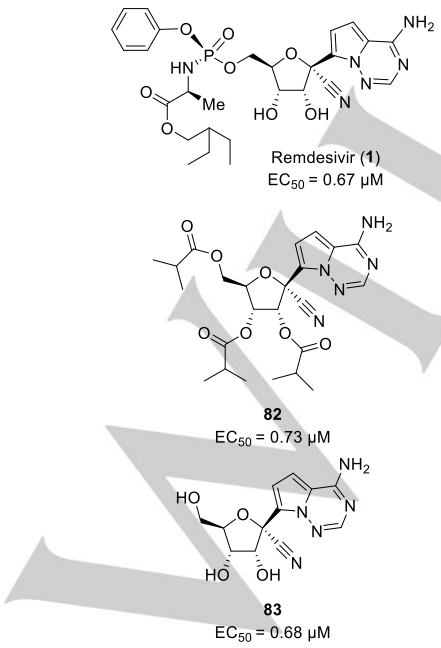

Figure 44. RdRp Nucleoside Inhibitors

improvement by day 15 and those in the remdesivir group had lower mortality estimates by day 15 and day 29.[36]

Based on the evidence from many clinical trials, remdesivir was FDA approved for use in hospitalized individuals infected with SARS-CoV-2 on October 22, 2020.[121] However, remdesivir is currently only available as an intravenous injection and must be administered in a health care setting making it less available to the general public. Research into an orally bioavailable analogue is underway in many laboratories. One study found

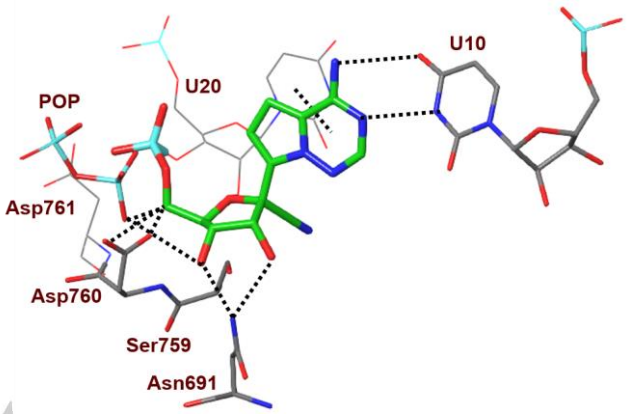

Figure 45. Remdesivir (green) bound RdRp (PDB 7BV2).

compound **82** (Figure 44), which is an oral prodrug of the remdesivir triol **83**.[122] This analogue displayed high oral bioavailability in two animal species including non-human primates.[122] Tested in VeroE6 cells against different strains of SARS-CoV-2 led to a range of EC_{50} values between 0.11 and 0.73 μ M for GS-621763 and no appreciable cytotoxicity.[123] Interestingly, it was also observed that treatment blocked viral transmission between untreated direct-contact animals.

Additionally, favipiravir (**84**, Figure 46) has also been tested for its activity against SARS-CoV-2 RdRp and is currently undergoing clinical trials.[124,125,126] Favipiravir is a potent influenza RdRp inhibitor that is intracellularly converted to its active triphosphate metabolite.[115] It has been shown to have activity against several RNA viruses, and has displayed efficacy in VeroE6 cells infected with SARS-CoV-2 with an EC_{50} of 61.88 μM and no appreciable cytotoxicity observed.[115,127] Recently the structure of SARS-CoV-2 RdRp in the presence of favipiravir-RTP was published.[128]

Molnupiravir, (**3**) an orally bioavailable RdRp acting drug developed in conjunction with Emory University, Ridgeback Biotherapeutics, and Merck is also currently undergoing phase III clinical trials and received an approval for EUA.[129,130] It was originally developed for use against influenza, but has demonstrated broad-spectrum antiviral activity, a good safety profile, tolerability, and oral bioavailability in humans.[130] The mechanism of action for molnupiravir is slightly different than that for remdesivir. Like remdesivir, molnupiravir is converted to its active form, β-D-N^4- hydroxycytidine triphosphate, in cells.[114,130] This active form is a substrate for viral RNA polymerase, which subsequently allows incorporation into the viral RNA. Molnupiravir is incorporated into the RNA strand in place of cytidine triphosphate or uridine triphosphate, which forms stable base pairs with either guanine or adenine.[114] Utilizing this erroneous RNA as a template results in molnupiravir directing the incorporation of guanine or adenine, and thus mutated RNA

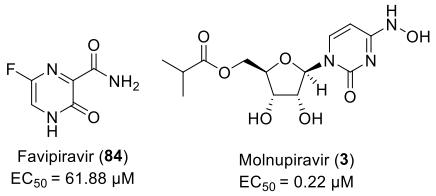

Figure 46. Inhibitors **3** and **84.**

products.[114] As these mutations accumulate, lethal mutagenesis occurs. Molnupiravir escapes detection from the viral proof-reading exonuclease via a couple of ways. First, it does not cause chain termination, and it is expected that its incorporation is not recognized by the viral proof-reading exonuclease as a misincorporation.[114] Additionally, this evasion could be due to the stability of M-G and M-A base pairing, which also does not promote RdRp backtracking.[114]

Studies utilizing molnupiravir and favipiravir in tandem have been reported and found this to be particularly effective in hamsters, and it was also observed that it largely reduces the transmission of the virus to uninfected individuals.[131] Due to the mechanism of action there has been cause for concern, among them possibilities of molnupiravir aiding in the emergence of variant coronaviruses. Despite the possible risks, a panel on the FDA voted 13-10 in favor of granting its emergency use authorization on November 30, 2021.

Since its EUA clinical data has shown that it is considerably less effective at reducing risk than was originally expected. Initial reports led researchers to believe molnupiravir would be closer to 50% effective, however, with more data becoming available only a 30% reduction in COVID-19 related hospitalization or death has been observed and reported.[85] It has been reported to effectively reduce omicron viral RNA in cultured lung epithelial cells by 70% with an estimated IC_{50} against wild type SARS-CoV-2 of 1.965 μM and 0.7556 μM against the omicron variant.[86]

The most successful RdRp inhibitors have been mentioned above; however, there is no shortage of weapons in the drug-repurposing arsenal. Galidesivir, ribavirin, sofosbuvir, and tenofovir have been reported to be under consideration.[115,123] Independently, an in silico drug repurposing study utilizing molecular docking and dynamics studies was conducted on over 30 compounds in which the ones to most tightly bind the active site of SARS-CoV-2 RdRp were found to be: remdesivir, favipiravir sofosbuvir, ribavirin, galidesivir, cefuroxime, tenofovir, and hydroxychloroquin.[132]

5.2 RdRp Non-Nucleoside Inhibitors

Unlike nucleoside inhibitors, non-nucleoside inhibitors are unencumbered by the proofreading activity of the coronavirus. Cen and coworkers reported a drug repurposing study and found a non-nucleoside RdRp inhibitor, corilagin **85** (Figure 47), which binds directly to RdRp and inhibits the polymerase activity in both cell-free and cell-based assays.[133] It fully resists the proofreading activity and potently inhibits SARS-CoV-2 infection with a low EC_{50}. Their work began with a virtual screening of over 15,000 compounds that culminated in the top 50 hits with strong binding energies being selected. These hits binding affinities were further validated through bio-layer interferometry binding assay. Of the initial 50 compounds, 6 showed direct SARS-CoV-2 RdRp binding. Corilagin showed the strongest RdRp binding affinity and was shown to effectively inhibit SARS-CoV-2 RdRp in Vero cells and showed moderate synergistic effects with remdesivir on inhibiting HCoV-OC43.[133]

Zandi and co-workers reported, two natural products, baicalein (**86**) and baicalin (**87**), displayed significant antiviral activity against SARS-CoV-2.[134] Through their cell-based and biochemical studies, both compounds were determined to act as RdRp inhibitors.

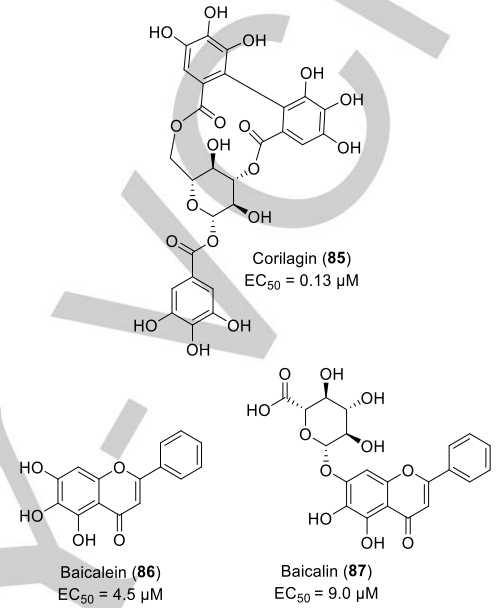

Figure 47. Non-Nucleoside RdRp Inhibitors **85-87.**

Antiviral activity was measured utilizing their previously established and optimized in vitro SARS-CoV-2 cell-based virus yield assay method and cytotoxicity was measured against Vero cells using a cell viability MTS assay.[135] Assays were completed utilizing remdesivir as a control, and none of the tested compounds exhibited any cytotoxicity. Baicalein displayed more potent activity in contrast with baicalin and was found to inhibit intracellular replication even when added up to 8 hours post infection. Both compounds did show significant effects on the early stages of SARS-CoV-2 replication through 6-8 hours post infection. The hypothesized mechanism of action is that these inhibitors act by binding to SARS-CoV-2 RdRp in a place other than the active site and that the mechanism of action for these natural products differ from that of remdesivir.[134]

6. Methyltransferase Inhibitors

Methyltransferase is an emerging target for drug design for antivirals of SARS-CoV-2, which contains two methyltransferases (MTase): Nsp14 and Nsp16. These enzymes are responsible for capping viral mRNAs, which is essential for transcription and avoiding the host's innate immune system. Capping ensures integrity of the viral RNA and consists of an N-methylated guanosine triphosphate and C2'-O-methyl-ribosyladenine.[136] It resembles the native mRNA of host cells, stabilizes the RNA, and ensures effective translation.[136] This also allows the viral RNA to

escape detection of the host's innate immune system by mimicking the natural mRNA in host cells.

Both enzymes bind Nsp10, which is a stable monomeric protein with no currently identified individual purpose. It is mainly known to stabilize the S-adenosylmethionine (SAM)-binding pockets of both Nsp14 and Nsp16.[136] Both Nsps are SAM-dependent MTases. Nsp14 is responsible for methylation of the cap on the guanine of the GTP, N^7-MTase, and exonuclease activities.[137] Association with Nsp14 stimulates exonuclease activity, but does not affect the MTase activity.[136] There is currently no crystal structure for SARS-CoV-2 Nsp14 MTase, although there is a solved crystal structure for the Nsp14 methyltransferase of SARS-CoV, which is expected to have a 94.9% homogeny with the SARS-CoV-2 Nsp14 methyltransferase.[138]

Nsp16 is a 7-methylguanine-triphosphate-adenosine specific, 2'-O-MTase, whose activation occurs via binding cofactor Nsp10.[137] Nsp16 is responsible for the methylation of the C2' hydroxyl group of the following nucleotide. The crystal structure of Nsp10-Nsp16 complex bound to the inhibitor sinefungin has been reported and solved by Boura and co-workers as well as the high-resolution structures for Nsp16-Nsp10 heterodimers bound to SAM or sinefungin reported by Rosas-Lemus and collaborators.[136,137] Inhibitors that prevent methyltransferase activity either by competitively binding the native substrate, SAM, or by blocking interactions with Nsp10 can be developed, and in fact, several small molecules have been reported in the last year.

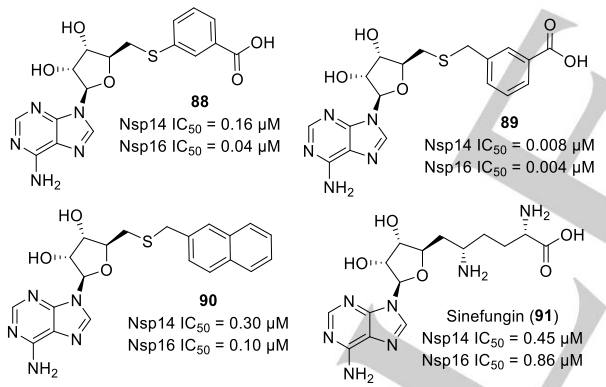

Figure 48. MTase Nsp14 and Nsp16 Inhibitors **88-91.**

Jaudzems and co-workers reported a series of Nsp14 and Nsp16 inhibitors designed utilizing bioisosteric substitution of the sulfonium and amino acid side chains of the cosubstrate SAM.[139] Three of their most potent compounds (**88**-**91**) are shown in Figure 48, and sinefungin (**91**) was utilized as a control. It was found that replacing the sulfonium with a thioether resulted in an increase in potency. This is said to indicate that conformational flexibility and bulkiness is more essential for activity rather than the positive charge.[139] An aromatic or heteroaromatic group in place of the aliphatic amino acid side chain also improved potency. Interestingly, it was noted that the improvements were more dramatic for Nsp16 over Nsp14, and this was hypothesized to be due to the ability for the inhibitor's adenine fragment to bind Nsp16 in a conformation more similar to SAM than in Nsp14.

In order to determine inhibitor selectivity, their derivatives were also tested for their inhibition against human glycine *N*-methyltransferase (GNMT). It was found that the inhibitors are also potent inhibitors of GNMT and are in fact not selective for SARS-CoV-2 methyltransferase. Despite this, the compounds exhibited no cytotoxicity in mouse embryo fibroblast, human liver cancer, and adenocarcinomic human alveolar basal epithelial cell lines. From there, it was suspected there was an issue with compound permeability. This was then tested by determining cell lysates and culture media by mass spectrometry and it was indeed found that the lysates were low and often below the detection limit.[139] Thus, further optimization of this class of compounds is required to improve selectivity and lipophilicity. Nencka and collaborators reported a series of Nsp14

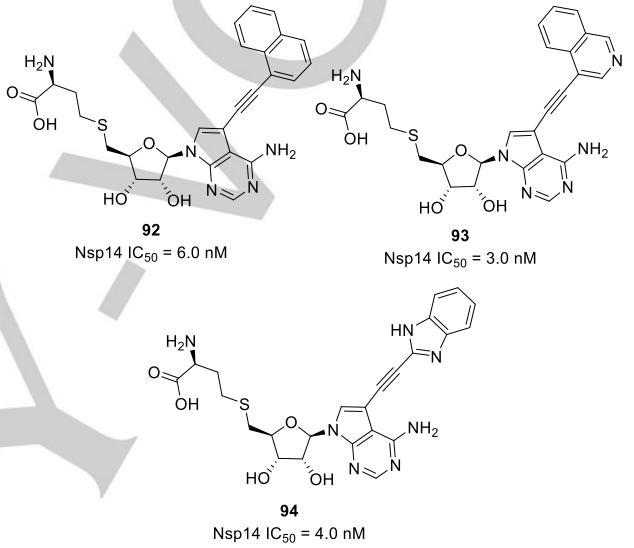

Figure 49. MTase Nsp 14 Inhibitors **92-94**

methyltransferase inhibitors created on structure based design of SARS-CoV-2 Nsp14 ligands.[138] The structure and activity of the most active compounds, **92**-**94**, are shown in Figure 49. Inhibitor design was derived from a model of SARS-CoV-2 bound SAM based on crystallized SARS-CoV Nsp14. It was hypothesized that aromatic systems would be able to interact significantly with the aromatic amino acid residues and Arg289 through cation-π interactions.[138]

The mechanism of action of **92** and **93** were investigated and it was shown that both derivatives compete with SAM, but are RNA noncompetitive Nsp14 inhibitors. Inhibitor selectivity was also investigated against 33 human RNA-, DNA-, and protein-MTases. No significant inhibition was observed from 20 of the protein lysine-MTases, but both compounds did exhibit some inhibitory activity against other MTases.

Debart and co-workers reported their synthesis and evaluation of nucleoside-derived inhibitors against SARS-CoV-2 Nsp14 MTase, which catalyzes the transfer of the SAM methyl to the N7-guanosine cap.[140] They tested 39 SAM analogues, of which 7 were found to exhibit double-digit nanomolar activity against the methyltransferase.[140] Three of the most potent discovered inhibitors stabilized Nsp14, and the best inhibitor showed high selectivity over human RNA N7-methyltransferase. They set out to synthesize smaller, efficient molecules with the

ability to enter cells. Several regions were varied as part of their SAR study, shown in red in compound **95** in Figure .

Three regions focused on included the linker between the deoxyadenosine and the phenyl ring, substituents on the phenyl

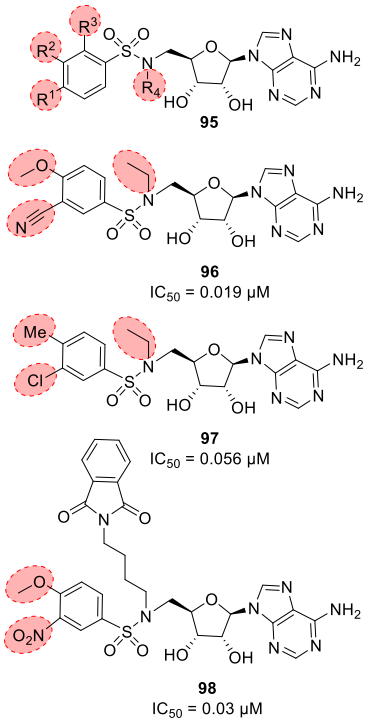

Figure 50. Nsp14 Inhibitors **95-98.**

ring, and functionalization of the 5'-nitrogen on the nucleoside. The sulfonamide linker proved crucial, as it was replaced with an amide and lost inhibitory activity. Substitution on the sulfonamide nitrogen with an ethyl (R^4) was tested as it was expected to improve hydrophobicity and cellular penetration. Further investigations involved attaching a butyl chain with various terminal groups, such as an ethyl ester, acetate, phthalate, or phthalimide. An increase in potency was experienced when R^1 was varied to a nitro, which was then changed to a nitrile (**96**) as the nitro is expected to have increased mutagenic potential and the nitrile is expected to interact similarly with Arg310.[140] Several compounds were also synthesized incorporating hydrophobic substituents at R^2 in order to fill the hydrophobic pocket. The most active compounds, **96**-**98**, are shown in Figure 50.

Biological activity was determined for all synthesized compounds, and only 8 were found to be not active against SARS-CoV-2 Nsp14. At least 65% inhibition was displayed for all of the active compounds, 11 of which displayed better activity than the control compound, sinefungin.[140] Further investigation into the mechanism of action showed that the most active compound, **96**, is a SAM-competitive inhibitor for Nsp14. Specificity of this inhibitor was also tested in dose response assays containing N7-MTase from vaccinia virus, 2'-O-MTases from Dengue virus, vaccinia virus, SARS-CoV-2, and human RNA N7-MTase (hRNMT). No inhibition was found for any of the viral MTases up to 50 μM, and against hRNMT at 50 μM compound **96** had an IC_{50} of 52.8 μM.[140] Thus, a high selectivity for SARS-CoV-2 Nsp14 was observed.

7. Other Therapies for SARS-Cov-2

Prevention of viral entry into the cell has also proven to be an active area of research. There are several ways to prevent this: ACE-2 blockers, host cell protease inhibitors such as transmembrane serine protease 2 (TMPRSS2), inhibitors of viral fusion, and monoclonal antibodies directed towards the spike protein. Entry inhibitors targeting any of the steps of the viral entry process into cells are an emerging area of interest. It is known that the viral spike protein must bind to the angiotensin-converting enzyme 2 (ACE2) cell receptor in order to initiate cell entry. The spike protein has been most heavily investigated for vaccine production, but viral entry inhibitors have also been investigated to prevent this process.

Monoclonal antibodies have been investigated and given emergency use authorization for the treatment of COVID-19. Monoclonal antibodies developed center around the spike protein and utilize this to prevent viral entry into the cell.[141] A risk reduction of 70-85% against mild to moderate COVID-19 infection in outpatient settings has been reported.[141] Unfortunately, as treatment effectiveness revolves around the spike protein, new variants with extensive mutations in the spike protein may be less susceptible to current antibody treatment methods. Treatment is also more intensive as antibodies are administered as an intravenous injection, which must occur in a health care setting. In addition to antibodies, some small molecules have also been shown to inhibit the spike protein and ACE2 interaction.[142]

Buchwald and co-workers reported a series of small-molecule inhibitors of the COVID Spike ACE2 protein-protein interaction (PPI) to prevent viral cell entry.[143] Interestingly they chose to investigate several dyes and novel drug-like compounds

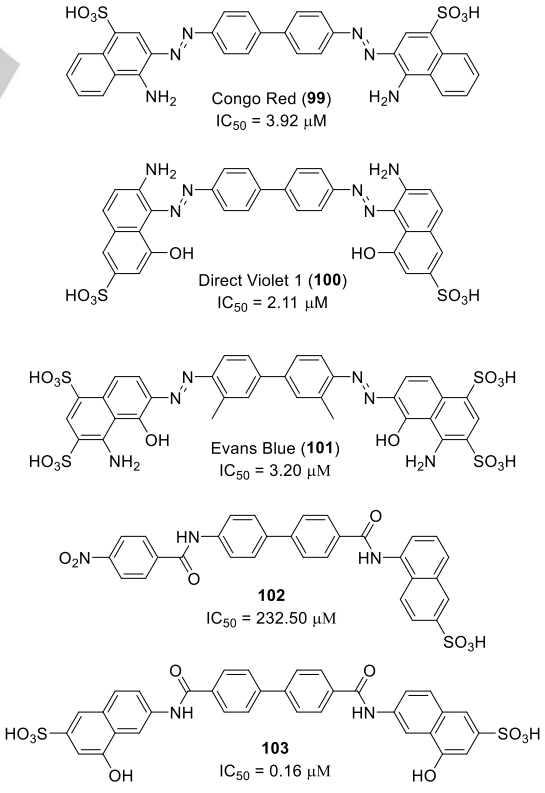

Figure 51. Dye based PPI Inhibitors, **99-103**

derived from these dyes, stemming from a screening of their compound library. The depicted compounds **99**-**103** (Figure 51) showed the most promising results for preventing PPI of ACE2 and the spike protein of SARS-CoV-2. They also investigated the binding partner for these compounds utilizing a thermal shift assay, and it was determined that the compounds were targeting the coronavirus spike protein.[143] These promising results can be further expanded upon and optimized in the future.

Coronaviruses require calcium ions to coordinate amino acid residues within the conserved fusion peptide of the spike protein to enter cells. Daniel and co-workers investigated calcium-channel-blocker drugs to inhibit SARS-CoV-2 entry into cells.[144] Cell lines tested included the most common VeroE6 cell line as well as epithelial lung cells. A total of five drugs from the different classes were chosen and tested for their activity. The most active and least cytotoxic compounds were found to be nifedipine (**104**, Figure 52) and felodipine (**105**), with nifedipine exhibiting no noticeable cytotoxicity. These compounds are expected to inhibit viral entry into the cell via calcium ion chelation; however, this hypothesis needs to undergo further testing for confirmation as it is possible they could inhibit viral spread at other stages of the life cycle.[144]

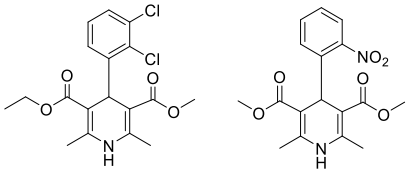

Figure 52. Calcium ion blockers, **104-105**

Hall and collaborators reported a virtual screen of 120 different compounds and found two novel chemotypes of entry inhibitors that target the fusion peptide of SARS-CoV-2.[145]

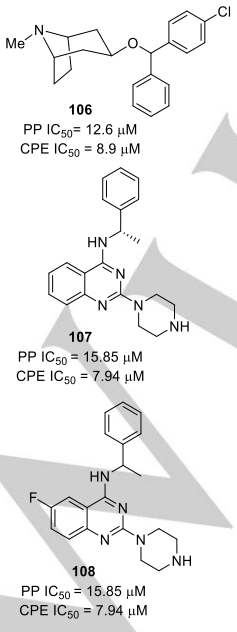

Figure 53. Entry Inhibitors **106-108**

Selected compounds were tested in SARS-CoV-2 PPI entry assay and the live CPE assay. Two chemotypes predominated and displayed good activity in both assays shown in Figure 53. Compound **106** is an antihistamine and quinazoline **107** is a positive allosteric modulator for thyrotropin receptor. Interestingly quinazoline **107** is of a chemotype that had previously shown no antiviral activity. Derivatives of quinazoline were further investigated and the most potent non-cytotoxic analogue with an IC_{50} of 15.8 μM was derivative **108**.

Kinase inhibitors that interfere with the phosphorylation of proteins essential for cell growth, signaling, and survival are another proposed area of treatment for COVID-19. These inhibitors can prevent phosphorylation of proteins vital to the immune activation and inflammation, causing immunosuppression and less severe symptoms.[146,147] Janus

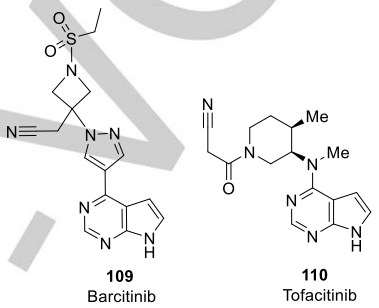

Figure 54. Kinase inhibitors baricitinib and tofacitinib

kinase (JAK) inhibitors baricitinib **109** (Figure 54) and tofacininb **110** have been investigated for possible treatment of COVID-19.[148] Baricitinib received FDA approval on May 11, 2022 for the treatment of COVID-19 in hospitalized adults requiring supplemental oxygen, non-invasive or invasive mechanical ventilation, or extracorporeal membrane oxygen.[148,150] Baricitinib in particular has a possibility of having direct antiviral activity via viral endocytosis interference, which would prevent SARS-CoV-2 from entering and infecting cells.[147] Clinical trials involving baricitinib and remdesivir are currently underway.[151]

8. Conclusion

The emergence of the COVID-19 pandemic at the end of 2019 shocked the world and demanded the most serious attention for the development of efficacious treatment of COVID-19. As a consequence, scientists across the globe plunged into developing vaccines and antiviral drugs in an unprecedented manner. The development of COVID-19 vaccines is a remarkable achievement. Never before have such safe and effective vaccines been developed with such rapid speed. Certainly, the COVID-19 vaccine's success will change the future of vaccine science. Vaccines will play a critical role in terminating the current pandemic.

However, development of effective antiviral drugs with proven efficacy is critically important to save lives and reduce morbidity and hospitalization. The groundwork for the development of small molecule antivirals for COVID-19 treatment has been nicely laid in the context of drug treatment options for both SARS-CoV infections in 2003 and MERS-CoV infections in 2012. Past and present research on coronavirus replication

unveiled numerous biochemical targets for antiviral development. Many different strategies and approaches are being pursued, which include de novo drug development, drug repurposing, and monoclonal antibody therapy development. In this review, we have outlined recent approaches to small molecule drug development targeting different pathways to block viral replication. Drug repurposing efforts led to the development and approval of remdesivir and molnupiravir, both drug targets viral RdRp. Remdesivir is an intravenous drug and molnupiravir is an oral therapy. Development of protease inhibitors have had much success for the treatment of HIV/AIDS and HCV infections. Early work on the coronavirus protease provided a much needed head start with lead structures and medicinal chemistry development efforts on SARS-CoV 3CLpro and SARS-CoV-PLpro targets. The development of the first FDA approved orally active SARS-CoV-2 3CLpro inhibitor drug is a very important achievement. Other new and effective treatments are needed to deal with side effects, resistance, and emerging variants. We hope the present review will further stimulate the development of effective broad-spectrum antivirals against COVID and emerging variants of SARS-CoV-2.

ABBREVIATIONS USED: 3CLpro, 3-chymotrypsin-like protease; 3CLpro, 3-chymotrypsin-like protease (3CLpro); ACE2, angiotensin-converting enzyme 2; ADMET, absorption, distribution, metabolism, excretion, toxicity; AIDS, acquired immunodeficiency syndrome; CPE, cytopathic effect; CYP, cytochrome P450 enzymes; DNA, deoxyribonucleic acid; FRET, Fluorescence Resonance Energy Transfer; GTP, guanosine triphosphate; GNMT, glycine *N*-methyltransferase; HCoVs, human coronaviruses; HCV, hepatitis C virus; NSP3, non-structural protein 3; HIV, human immunodeficiency virus; MERS-CoV, Middle east respiratory syndrome coronavirus; MHV coronavirus, Mouse Hepatitis Virus coronavirus; Mpro, main protease; MTase, methyltransferases; NSAID, nonsteroidal anti-inflammatory agents; PDB, protein data base; PLpro, papain-like protease; RdRp, RNA-dependent RNA polymerase; RNA, ribonucleic acid; SAM, S-adenosylmethionine; SARS-CoV-2, severe acute respiratory syndrome coronavirus 2.

Acknowledgements

The research was supported in part by grants from the National Institute of Allergy and Infectious Diseases, National Institutes of Health (A.K.G., AI158649 and A.D.M., contract No. HHSN272201700060C). The present work was also supported by a grant for Development of Novel Drugs for Treating COVID-19 from the Intramural Research Program of National Center for Global Health and Medicine (H.M., 19A3001 and S.H., 20A2001D), in part by Japan Agency for Medical Research and Development (AMED) (H.M., 20fk0108257). The authors acknowledge support from the Purdue Center for Cancer Research, NIH grant P30 CA023168 for use of the shared NMR and mass spectrometry facilities. This research used resources of the Advanced Photon Source, a U.S. Department of Energy (DOE) Office of Science User Facility operated for the DOE Office of Science by Argonne National Laboratory under Contract No. DE-AC02-06CH11357. Use of the LS-CAT Sector 21 was supported by the Michigan Economic Development Corporation and the Michigan Technology Tri-Corridor (Grant 085P1000817).

Keywords: antiviral drugs • COVID-19 • coronavirus • drug design • inhibitors • protein X-ray structures • SARS-CoV-2

References

[1] F. Wu, S. Zhao, B. Yu, Y.-M. Chen, W. Wang, Z.-G. Song, Y. Hu, Z.-W. Tao, J.-H. Tian, Y.-Y. Pei, M.-L. Yuan, Y.-L.; Zhang, F.-H. Dai, Y. Liu, Q.-M. Wang, J.-J. Zheng, L. Xu, E. C. Holmes, Y.-Z. Zhang, *Nature* **2020**, *579*, 265–269.

[2] P. Zhou, X.-L. Yang, X.-G. Wang, B. Hu, L. Zhang, W. Zhang, H.-R. Si, Y. Zhu, B. Li, C.-L. Huang, H.-D. Chen, J. Chen, Y. Luo, H. Guo, R.-D. Jiang, M.-Q. Liu, Y. Chen, X.-R. Shen, X. Wang, X.-S. Zheng, K. Zhao, Q.-J. Chen, F. Deng, L.-L. Liu, B. Yan, F.-X. Zhan, Y.-Y. Wang, G.-F. Xiao, Z.-L. Shi, *Nature* **2020**, *579*, 270–273.

[3] V. Zoumpourlis, M. Goulielmaki, E. Rizos, S. Baliou, D. Spandidos, [Comment] The COVID-19 Pandemic as a Scientific and Social Challenge in the 21st Century. *Mol. Med. Rep.* **2020**.

[4] *WHO-convened global study of origins of SARS-CoV-2: China Part*. https://www.who.int/publications-detail-redirect/who-convened-global-study-of-origins-of-sars-cov-2-china-part.

[5] *Coronavirus COVID-19 (2019-nCoV)*. https://gisanddata.maps.arcgis.com/apps/dashboards/bda7594740fd40299423467b48e9ecf6.

[6] C. Huang, Y. Wang, X. Li, L. Ren, J. Zhao, Y. Hu, L. Zhang, G. Fan, J. Xu, X. Gu, Z. Cheng, T. Yu, J. Xia, Y. Wei, W. Wu, X. Xie, W. Yin, H. Li, M. Liu, Y. Xiao, H. Gao, L. Guo, J. Xie, G. Wang, R. Jiang, Z. Gao, Q. Jin, J. Wang, B. Cao, *The Lancet* **2020**, *395*, 497–506.

[7] S. Kim, *J. Microbiol. Biotechnol.* **2022**, *32*, 1–5.

[8] L. Rodrigues, R. Bento Cunha, T. Vassilevskaia, M. Viveiros, C. Cunha, *Molecules* **2022**, *27*, 2723.

[9] A. K. Ghosh, M. Brindisi, D. Shahabi, M. E. Chapman, A. D. Mesecar, *ChemMedChem* **2020**, *15*, 907–932.

[10] Y. M. Báez-Santos, S. E. St. John, A. D. Mesecar, *Antiviral Res.* **2015**, *115*, 21–38.

[11] (a) J. Cui, F. Li, Z.-L. Shi, *Nat. Rev. Microbiol.* **2019**, *17*, 181–192; (b) A. Zumla, D. S. Hui, S. Perlman, *The Lancet* **2015**, *386*, 995–1007.

[12] (a) A. N. Vlasova, A. Diaz, D. Damtie, L. Xiu, T. H. Toh, J. S. Lee, L. J. Saif, G. C. Gray, *Clin. Infect. Dis.* **2022**, *74*, 446-454; (b) A. N. Vlasova, T. H. Toh, J. S. Lee, Y. Poovorawan, P. Davis, M. S. P. Azevedo, J. A. Lednicky, L. J. Saif, G. C. Gray, *Emerg. Microbes Infect.* **2022**, *11*, 699-702.

[13] J. S. M. Peiris, Y. Guan, K. Y. Yuen, *Nature Medicine.* **2004**, *10*, S88–S97.

[14] K. Pyrc, B. Berkhout, L. van der Hoek, *Expert Rev. Anti Infect. Ther.* **2007**, *5*, 245–253.

[15] C. Drosten, S. Günther, W. Preiser, S. van der Werf, H.-R. Brodt, S. Becker, H. Rabenau, M. Panning, L. Kolesnikova, R. A. M. Fouchier, A. Berger, A.-M. Burguière, J. Cinatl, M. Eickmann, N. Escriou, K. Grywna, S. Kramme, J.-C. Manuguerra, S. Müller, V. Rickerts, M. Stürmer, S. Vieth, H.-D. Klenk, A. D. M. E. Osterhaus, H. Schmitz, H. W. Doerr, *N. Engl. J. Med.* **2003**, *348*, 1967–1976.

[16] M. D. Christian, S. M. Poutanen, M. R. Loutfy, M. P. Muller, D. E. Low, *Clin. Infect. Dis.* **2004**, *38*, 1420–1427.

[17] R. Hilgenfeld, M. Peiris, *Antiviral Res.* **2013**, *100*, 286–295.

[18] I. Eckerle, M. A. Müller, S. Kallies, D. N. Gotthardt, C. Drosten, *Virol. J.* **2013**, *10*, 359.

[19] D. Butler, *Nature* **2015**, *522*, 139–140.

[20] J. S. Morse, T. Lalonde, S. Xu, W. Liu, *Learning from the Past: Possible Urgent Prevention and Treatment Options for Severe Acute Respiratory Infections Caused by 2019-NCoV*; preprint; Chemistry, 2020.

[21] P. V. Baranov, C. M. Henderson, C. B. Anderson, R. F. Gesteland, J. F. Atkins, M. T. Howard, *Virology* **2005**, *332*, 498–510.

[22] A. E. Gorbalenya, E. J. Snijder, J. Ziebuhr, *J. Gen. Virol.* **2000**, *81*, 853–879.

[23] X. Xu, *Nucleic Acids Res.* **2003**, *31*, 7117–7130.

[24] A. Dömling, L. Gao, *Chem* **2020**, *6*, 1283–1295.
[25] T. Pillaiyar, M. Manickam, V. Namasivayam, Y. Hayashi, S.-H. Jung, *J. Med. Chem.* **2016**, *59*, 6595–6628.
[26] D. Forni, R. Cagliani, M. Clerici, M. Sironi, *Trends Microbiol.* **2017**, *25*, 35–48.
[27] R. L. Graham, J. S. Sparks, L. D. Eckerle, A. C. Sims, M. R. Denison, *Virus Res.* **2008**, *133*, 88–100.
[28] A. Kanjanahaluethai, Z. Chen, D. Jukneliene, S. C. Baker, *Virology* **2007**, *361*, 391–401.
[29] V. Thiel, K. A. Ivanov, Á. Putics, T. Hertzig, B. Schelle, S. Bayer, B. Weißbrich, E. J. Snijder, H. Rabenau, H. W. Doerr, A. E. Gorbalenya, J. Ziebuhr, *J. Gen. Virol.* **2003**, *84*, 2305–2315.
[30] H. Yang, M. Yang, Y. Ding, Y. Liu, Z. Lou, Z. Zhou, L. Sun, L. Mo, S. Ye, H. Pang, G. F. Gao, K. Anand, M. Bartlam, R. Hilgenfeld, Z. Rao, *Proc. Natl. Acad. Sci.* **2003**, *100*, 13190–13195.
[31] K. Ratia, K. S. Saikatendu, B. D. Santarsiero, N. Barretto, S. C. Baker, R. C. Stevens, A. D. Mesecar, *Proc. Natl. Acad. Sci.* **2006**, *103*, 5717–5722.
[32] Y. M. Baez-Santos, A. M. Mielech, X. Deng, S. Baker, A. D. Mesecar, *J. Virol.* **2014**, *88*, 12511–12527.
[33] M. B. Serafin, A. Bottega, V. S. Foletto, T. F. da Rosa, A. Hörner, R. Hörner, *Int. J. Antimicrob. Agents* **2020**, *55*, 105969.
[34] W. Zheng, W. Sun, A. Simeonov, *Br. J. Pharmacol.* **2018**, *175*, 181–191.
[35] A. J. Brown, J. J. Won, R. L. Graham, K. H. Dinnon, A. C. Sims, J. Y. Feng, T. Cihlar, M. R. Denison, R. S. Baric, T. P. Sheahan, *Antiviral Res.* **2019**, *169*, 104541.
[36] J. H. Beigel, K. M. Tomashek, L. E. Dodd, A. K. Mehta, B. S. Zingman, A. C. Kalil, E. Hohmann, H. Y. Chu, A. Luetkemeyer, S. Kline, D. Lopez de Castilla, R. W. Finberg, K. Dierberg, V. Tapson, L. Hsieh, T. F. Patterson, R. Paredes, D. A. Sweeney, W. R. Short, G. Touloumi, D. C. Lye, N. Ohmagari, M. Oh, G. M. Ruiz-Palacios, T. Benfield, G. Fätkenheuer, M. G. Kortepeter, R. L. Atmar, C. B. Creech, J. Lundgren, A. G. Babiker, S. Pett, J. D. Neaton, T. H. Burgess, T. Bonnett, M. Green, M. Makowski, A. Osinusi, S. Nayak, H. C. Lane, *N. Engl. J. Med.* **2020**, *383*, 1813–1826.
[37] R. T. Eastman, J. S. Roth, K. R. Brimacombe, A. Simeonov, M. Shen, S. Patnaik, M. D. Hall, *ACS Cent. Sci.* **2020**, *6*, 672–683.
[38] Remdesivir for the Treatment of Covid-19 — Preliminary Report. *N. Engl. J. Med.* **2020**, *383*, 992–994.
[39] V. C. Yan, F. L. Muller, *Antimicrob. Agents Chemother.* **2021**, *65*, e01117-21.
[40] *WHO recommends against the use of remdesivir in COVID-19 patients*. https://www.who.int/news-room/feature-stories/detail/who-recommends-against-the-use-of-remdesivir-in-covid-19-patients.
[41] R. L. Gottlieb, C. E. Vaca, R. Paredes, J. Mera, B. J. Webb, G. Perez, G. Oguchi, P. Ryan, B. U. Nielsen, M. Brown, A. Hidalgo, Y. Sachdeva, S. Mittal, O. Osiyemi, J. Skarbinski, K. Juneja, R. H. Hyland, A. Osinusi, S. Chen, G. Camus, M. Abdelghany, S. Davies, N. Behenna-Renton, F. Duff, F. M. Marty, M. J. Katz, A. A. Ginde, S. M. Brown, J. T. Schiffer, J. A. Hill, *N. Engl. J. Med.* **2022**, *386*, 305–315.
[42] P.-V. Ennezat, Outpatient Remdesivir to Prevent Progression to Severe Covid-19. *N. Engl. J. Med.* **2022**, *386*, 1094–1094.
[43] W. Fischer, J. J. Eron, W. Holman, M. S. Cohen, L. Fang, L. J. Szewczyk, T. P. Sheahan, R. Baric, K. R. Mollan, C. R. Wolfe, E. R. Duke, M. M. Azizad, K. Borroto-Esoda, D. A. Wohl, A. J. Loftis, P. Alabanza, F. Lipansky, W. P. Painter, *Molnupiravir, an Oral Antiviral Treatment for COVID-19*; preprint; Infectious Diseases (except HIV/AIDS), 2021.
[44] A. Jayk Bernal, M. M. Gomes da Silva, D. B. Musungaie, E. Kovalchuk, A. Gonzalez, V. Delos Reyes, A. Martín-Quirós, Y. Caraco, A. Williams-Diaz, M. L. Brown, J. Du, A. Pedley, C. Assaid, J. Strizki, J. A. Grobler, H. H. Shamsuddin, R. Tipping, H. Wan, A. Paschke, J. R. Butterton, M. G. Johnson, C. De Anda, *N. Engl. J. Med.* **2022**, *386*, 509–520.
[45] Commissioner, O. of the. *Coronavirus (COVID-19) Update: FDA Authorizes Additional Oral Antiviral for Treatment of COVID-19 in Certain Adults*. FDA. https://www.fda.gov/news-events/press-announcements/coronavirus-covid-19-update-fda-authorizes-additional-oral-antiviral-treatment-covid-19-certain.
[46] EUA 105 Pfizer Paxlovid LOA.
[47] D. R. Owen, C. M. N. Allerton, A. S. Anderson, L. Aschenbrenner, M. Avery, S. Berritt, B. Boras, R. D. Cardin, A. Carlo, K. J. Coffman, A. Dantonio, L. Di, H. Eng, R. Ferre, K. S. Gajiwala, S. A. Gibson, S. E. Greasley, B. L. Hurst, E. P. Kadar, A. S. Kalgutkar, J. C. Lee, J. Lee, W. Liu, S. W. Mason, S. Noell, J. J. Novak, R. S. Obach, K. Ogilvie, N. C. Patel, M. Pettersson, D. K. Rai, M. R. Reese, M. F. Sammons, J. G. Sathish, R. S. P. Singh, C. M. Steppan, A. E. Stewart, J. B. Tuttle, L. Updyke, P. R. Verhoest, L. Wei, Q. Yang, Y. Zhu, *Science* **2021**, *374*, 1586-1593.
[48] A. K. Ghosh, K. Xi, M. E. Johnson, S. C. Baker, A. D. Mesecar, Progress in Anti-SARS Coronavirus Chemistry, Biology and Chemotherapy. In *Annual Reports in Medicinal Chemistry*; Elsevier, 2006; Vol. 41, pp 183–196.
[49] *Pfizer's Novel COVID-19 Oral Antiviral Treatment Candidate Reduced Risk of Hospitalization or Death by 89% in Interim Analysis of Phase 2/3 EPIC-HR Study | Pfizer*. https://www.pfizer.com/news/press-release/press-release-detail/pfizers-novel-covid-19-oral-antiviral-treatment-candidate.
[50] J. Hsu, H.-C. Wang, G.-W. Chen, S.-R. Shih, *Curr. Pharm. Des.* **2006**, *12*, 1301–1314.
[51] W. Zhu, Z. Shyr, D. C. Lo, W. Zheng, *J. Pharmacol. Exp. Ther.* **2021**, *378*, 166–172.
[52] M. M. Prokofjeva, S. N. Kochetkov, V. S. Prassolov, *Acta Naturae* **2016**, *8*, 23–32.
[53] N. C. Pedersen, Y. Kim, H. Liu, A. C. Galasiti Kankanamalage, C. Eckstrand, W. C. Groutas, M. Bannasch, J. M. Meadows, K.-O. Chang, *J. Feline Med. Surg.* **2018**, *20*, 378–392.
[54] K. Sharun, R. Tiwari, K. Dhama, *Ann. Med. Surg.* **2021**, *61*, 122–125.
[55] V. Mody, J. Ho, S. Wills, A. Mawri, L. Lawson, M. C. C. J. C. Ebert, G. M. Fortin, S. Rayalam, S. Taval, *Commun. Biol.* **2021**, *4*, 93.
[56] H. Wang, S. He, W. Deng, Y. Zhang, G. Li, J. Sun, W. Zhao, Y. Guo, Z. Yin, D. Li, L. Shang, *ACS Catal.* **2020**, *10*, 5871–5890.
[57] G. Macip, P. Garcia-Segura, J. Mestres-Truyol, B. Saldivar-Espinoza, G. Pujadas, S. Garcia-Vallvé, *Int. J. Mol. Sci.* **2021**, *23*, 259.
[58] A. K. Ghosh, K. Xi, K. Ratia, B. D. Santarsiero, W. Fu, B. H. Harcourt, P. A. Rota, S. C. Baker, M. E. Johnson, A. D. Mesecar, *J. Med. Chem.* **2005**, *48*, 6767–6771.
[59] A. K. Ghosh, K. Xi, V. Grum-Tokars, X. Xu, K. Ratia, W. Fu, K. V. Houser, S. C. Baker, M. E. Johnson, A. D. Mesecar, *Bioorg. Med. Chem. Lett.* **2007**, *17*, 5876–5880.
[60] R. P. Jain, H. I. Pettersson, J. Zhang, K. D. Aull, P. D. Fortin, C. Huitema, L. D. Eltis, J. C. Parrish, M. N. G. James, D. S. Wishart, J. C. Vederas, *J. Med. Chem.* **2004**, *47*, 6113–6116.
[61] S. Hattori, N. Higashi-Kuwata, H. Hayashi, S. R. Allu, J. Raghavaiah, H. Bulut, D. Das, B. J. Anson, E. K. Lendy, Y. Takamatsu, N. Takamune, N. Kishimoto, K. Murayama, K. Hasegawa, M. Li, D. A. Davis, E. N. Kodama, R. Yarchoan, A. Wlodawer, S. Misumi, A. D. Mesecar, A. K. Ghosh, H. Mitsuya, *Nat. Commun.* **2021**, *12*, 668.
[62] Y. Kim, S. Lovell, K.-C. Tiew, S. R. Mandadapu, K. R. Alliston, K. P. Battaile, W. C. Groutas, K.-O. Chang, *J. Virol.* **2012**, *86*, 11754–11762.
[63] Y. Kim, V. Shivanna, S. Narayanan, A. M. Prior, S. Weerasekara, D. H. Hua, A. C. G. Kankanamalage, W. C. Groutas, K.-O. Chang, *J. Virol.* **2015**, *89*, 4942–4950.
[64] W. Vuong, C. Fischer, M. B. Khan, M. J. van Belkum, T. Lamer, K. D. Willoughby, J. Lu, E. Arutyunova, M. A. Joyce, H. A. Saffran, J. A. Shields, H. S. Young, J. A. Nieman, D. L. Tyrrell, M. J. Lemieux, J. C. Vederas, *Eur. J. Med. Chem.* **2021**, *222*, 113584.
[65] L. Fu, F. Ye, Y. Feng, F. Yu, Q. Wang, Y. Wu, C. Zhao, H. Sun, B. Huang, P. Niu, H. Song, Y. Shi, X. Li, W. Tan, J. Qi, G. F. Gao, *Nat. Commun.* **2020**, *11*, 4417.
[66] J. Lu, S. A. Chen, M. B. Khan, R. Brassard, E. Arutyunova, T. Lamer, W. Vuong, C. Fischer, H. S. Young, J. C. Vederas, M. J. Lemieux, *Front. Chem.* **2022**, *10*, 852210.
[67] C. Ma, M. D. Sacco, B. Hurst, J. A. Townsend, Y. Hu, T. Szeto, X. Zhang, B. Tarbet, M. T. Marty, Y. Chen, J. Wang, *Cell Res.* **2020**, *30*, 678–692.
[68] A. J. Prongay, Z. Guo, N. Yao, J. Pichardo, T. Fischmann, C. Strickland, J. Myers, P. C. Weber, B. M. Beyer, R. Ingram, Z. Hong, W. W. Prosise, L. Ramanathan, S. S. Taremi, T. Yarosh-Tomaine, R. Zhang, M. Senior, R.-S. Yang, B. Malcolm, A. Arasappan, F. Bennett, S. L. Bogen, K. Chen,

E. Jao, Y.-T. Liu, R. G. Lovey, A. K. Saksena, S. Venkatraman, V. Girijavallabhan, F. G. Njoroge, V. Madison, *J. Med. Chem.* **2007**, *50*, 2310–2318.

[69] B. A. Malcolm, R. Liu, F. Lahser, S. Agrawal, B. Belanger, N. Butkiewicz, R. Chase, F. Gheyas, A. Hart, D. Hesk, P. Ingravallo, C. Jiang, R. Kong, J. Lu, J. Pichardo, A. Prongay, A. Skelton, X. Tong, S. Venkatraman, E. Xia, V. Girijavallabhan, F. G. Njoroge, *Antimicrob. Agents Chemother.* **2006**, *50*, 1013–1020.

[70] (a) B. J. Anson; M. E. Chapman, E. K. Lendy; S. Pshenychnyi; R. T. D'Auila; K. J. F. Satchell; A. D. Mesecar. Broad-Spectrum inhibition of coronavirus main and papain-like proteases by HCV drugs. *Res. Square,* PREPRINT, https://doi.org.10.21203/rs.3.rs-26344/v1; (b) R. Oerlemans, A. J. Ruiz-Moreno, Y. Cong, N. Dinesh Kumar, M. A. Velasco-Velazquez, C. G. Neochoritis, J. Smith, F. Reggiori, M. R. Groves, A. Dömling, *RSC Med. Chem.* **2021**, *12*, 370–379.

[71] J. Qiao, Y.-S. Li, R. Zeng, F.-L. Liu, R.-H. Luo, C. Huang, Y.-F. Wang, J. Zhang, B. Quan, C. Shen, X. Mao, X. Liu, W. Sun, W. Yang, X. Ni, K. Wang, L. Xu, Z.-L. Duan, Q.-C. Zou, H.-L. Zhang, W. Qu, Y.-H.-P. Long, M.-H. Li, R.-C. Yang, X. Liu, J. You, Y. Zhou, R. Yao, W.-P. Li, J.-M. Liu, P. Chen, Y. Liu, G.-F. Lin, X. Yang, J. Zou, L. Li, Y. Hu, G.-W. Lu, W.-M. Li, Y.-Q. Wei, Y.-T. Zheng, J. Lei, S. Yang, *Science* **2021**, *371*, 1374–1378.

[72] (a) Y. Ma; K. S. Yang; Z. Z. Geng; Y. R. Alugubelli; N. Shaabani; E. C. Vatansever; X. R. Ma; C. C. Cho; K. Khatua; J. Xiao; L. R. Blankenship; G. Yu; B. Sankaran; P. Li; R. Allen; H. Ji; S. Xu; W. R. Liu. *E. J. Med. Chem.,* **2022**, *240*, 114570; (b) Y. R. Alugubelli; Z. Z. Geng; K. S. Yang; N. Shaabani; K. Khatua; X. R. Ma; E. C. Vatansever; C. C. Cho; Y. Ma; J. Xiao; L. R. Blankenship; G. Yu; B. Sankaran; P. Li; R. Allen; H. Ji; S. Xu; W. R. Liu. *E. J. Med. Chem.,* **2022**, *240*, 114596.

[73] B. X. Quan; H. Shuai; A. J. Xia; Y. Hou; R. Zeng; X. L. Liu; G. F. Lin; J. X. Qiao; W. P. Li; F. L. Wang; K. Wang; R. J. Zhou; T. T. Yuen; M. X. Chen; C. Yoon; M. Wu; S. Y. Zhang; C. Huang; Y. F. Wang; W. Yang; C. Tian; W. M. Li; Y. Q. Wei; K. Y. Yuen; J. Chan; J. Lei; H. Chu; S. Yang. *Nature Microbiology,* **2022**, *7*, 716-725.

[74] Z. Xia, M. Sacco, Y. Hu, C. Ma, X. Meng, F. Zhang, T. Szeto, Y. Xiang, Y. Chen, J. Wang, *ACS Pharmacol. Transl. Sci.* **2021**, *4*, 1408–1421.

[75] B. Bai; A. Belovodskiy; M. Hena; A. S. Kandadai; M. A. Joyce; H. A. Saffran; J. A. Shields; M. B. Khan; E. Arutyunova; J. Lu; S. K. Bajwa; D. Hockman; C. Fischer; T. Lamer; W. Vuong; M. J. van Belkum; Z. Gu; F. Lin; Y. Du; J. Xu; M. Rahim; H. S. Young; J. C. Vederas; D. L. Tyrrell; M. J. Lemieux; J. A. Nieman. *J. Med. Chem.* **2021**, *65*, 2905-2925.

[76] A. Krantz, L. J. Copp, P. J. Coles, R. A. Smith, S. B. Heard, *Biochemistry* **1991**, *30*, 4678–4687.

[77] R. A. Smith, L. J. Copp, P. J. Coles, H. W. Pauls, V. J. Robinson, R. W. Spencer, S. B. Heard, A. Krantz, *J. Am. Chem. Soc.* **1988**, *110*, 4429–4431.

[78] T. H. Eichhold, E. B. Hookfin, Y. O. Taiwo, B. De, K. R. Wehmeyer, *J. Pharm. Biomed. Anal.* **1997**, *16*, 459–467.

[79] E. H. Yeo, W. L. Goh, S. C. Chow, *Toxicol. Mech. Methods* **2018**, *28*, 157–166.

[80] R. L. Hoffman, R. S. Kania, M. A. Brothers, J. F. Davies, R. A. Ferre, K. S. Gajiwala, M. He, R. J. Hogan, K. Kozminski, L. Y. Li, J. W. Lockner, J. Lou, M. T. Marra, L. J. Mitchell, B. W. Murray, J. A. Nieman, S. Noell, S. P. Planken, T. Rowe, K. Ryan, G. J. Smith, J. E. Solowiej, C. M. Steppan, B. Taggart, *J. Med. Chem.* **2020**, *63*, 12725–12747.

[81] D. W. Kneller, G. Phillips, K. L. Weiss, Q. Zhang, M. A. Arnould C. B. Jonsson, S. Surendranathan, J. Parvathareddy, M. P. Blakeley, L. Coates, J. M. Louis, P. V. Bonnesen, A. Kovalevsky *Nat. Commun.* **2022**, *13*, 2268.

[82] Y. Zhao, C. Fang, Q. Zhang, R. Zhang, X. Zhao, Y. Duan, H. Wang, Y. Zhu, L. Feng, J. Zhao, M. Shao, X. Yang, L. Zhang, C. Peng, K. Yang, D. Ma, Z. Rao, H. Yang, *Protein Cell* **2022**, *13*, 689–693.

[83] *Pfizer unveils its oral SARS-CoV-2 inhibitor*. Chemical & Engineering News. https://cen.acs.org/acs-news/acs-meeting-news/Pfizer-unveils-oral-SARS-CoV/99/i13.

[84] J. Hammond, H. Leister-Tebbe, A. Gardner, P. Abreu, W. Bao, W. Wisemandle, M. Baniecki, V. M. Hendrick, B. Damle, A. Simón-Campos, R. Pypstra, J. M. Rusnak, *N. Engl. J. Med.* **2022**, *386*, 1397–1408.

[85] E. Mahase, *BMJ* **2021**, *375*, n2697.

[86] P. Li, Y. Wang, M. Lavrijsen, M. M. Lamers, A. C. de Vries, R. J. Rottier, M. J. Bruno, M. P. Peppelenbosch, B. L. Haagmans, Q. Pan, *Cell Res.* **2022**, *32*, 322–324.

[87] *EPIC-Peds: Study of Oral PF-07321332 (Nirmatrelvir)/Ritonavir in Nonhospitalized COVID-19 Pediatric Patients at Risk for Severe Disease - Full Text View - ClinicalTrials.gov*. https://clinicaltrials.gov/ct2/show/NCT05261139.

[88] D. K. D. Rai; I. Yurgelonis; P. McMonagle; H. A. Rothan; L. Hao; A. Gribenko; E. Titova; B. Kreiswirth; K. M. White; Y. Zhu.; A. S. Anderson.; R. D. Cardin. *Nirmatrelvir, an Orally Active Mpro Inhibitor, Is a Potent Inhibitor of SARS-CoV-2 Variants of Concern*; preprint; Microbiology, 2022.

[89] A. K. Ghosh, J. Raghavaiah, D. Shahabi, M. Yadav, B. J. Anson, E. K. Lendy, S. Hattori, N. Higashi-Kuwata, H. Mitsuya, A. D. Mesecar, *J. Med. Chem.* **2021**, *64*, 14702–14714.

[90] A. K. Ghosh, D. Shahabi, M. Yadav, S. Kovela, B. J. Anson, E. K. Lendy, C. Bonham, D. Sirohi, C. A. Brito-Sierra, S. Hattori, R. Kuhn, H. Mitsuya, A. D. Mesecar, *Molecules* **2021**, *26*, 5782.

[91] T. Pillaiyar; P. Flury; N. Krüger; H. Su; L. Schäkel; E. B. Da Silva; O. Eppler; T. Kronenberger; T. Jie; S. Luedtke; C. Rocha; K. Sylvester; M. R. Petry; J. H. McKerrow; A. Poso; S. Pöhlmann; M. Gütschow; A. J. O'Donoghue; Y. Xu; C. E. Müller; S. A. Laufer. *J. Med. Chem.,* **2022**, *65*, 9376-9395.

[92] J. Breidenbach; C. Lemke; T. Pillaiyar; L. Schäkel; G. A. Hamwi; M. Diett; R. Gedschold; N. Geiger; V. Lopez; S. Mirza; V. Namasivayam; A. C. Schiedel; K. Sylvester; D. Thimm; C. Vielmuth; L. P. Vu; M. Zyulina; J. Bodem; M. Gütschow; C. E. Müller. *Angew. Chem. Int. Ed.* **2021**, *60,* 10423-10429.

[93] C. Huang, Y. Wang, X. Li, L. Ren, J. Zhao, Y. Hu, L. Zhang, G. Fan, J. Xu, X. Gu, Z. Cheng, T. Yu, J. Xia, Y. Wei, W. Wu, X. Xie, W. Yin, H. Li, M. Liu, Y. Xiao, H. Gao, L. Guo, J. Xie, G. Wang, R. Jiang, Z. Gao, Q. Jin, J. Wang, B. Cao, *Lancet* **2020**, *395*, 497-506.

[94] H. Su, S. Yao, W. Zhao, Y. Zhang, J. Liu, Q. Shao, Q. Wang, M. Li, H. Xie, W. Shang, C. Ke, L. Feng, X. Jiang, J. Shen, G. Xiao, H. Jiang, L. Zhang, Y. Ye, Y. Xu, *Nat. Commun.* **2021**, *12*, 3623.

[95] D. Shcherbakov; D. Baev; M. Kalinin; A. Dalinger; V. Chirkova; S. Belenkaya; A. Khvostov; D. Krut'ko; A. Medved'ko; E. Volosnikova; E. Sharlaeva; D. Shanshin; T. Tolstikova; O. Yarovaya; R. Maksyutov; N. Salakhutdinov; S. Vatsadze. *ACS Med. Chem. Lett.* **2022**, *13*, 140-147.

[96] J. Jacobs, V. Grum-Tokars, Y. Zhou, M. Turlington, S. A. Saldanha, P. Chase, A. Eggler, E. S. Dawson, Y. M. Baez-Santos, S. Tomar, A. M. Mielech, S. C. Baker, C. W. Lindsley, P. Hodder, A. Mesecar, S. R. Stauffer, *J. Med. Chem.* **2013**, *56*, 534-546.

[97] N. Kitamura, M. D. Sacco, C. Ma, Y. Hu, J. A. Townsend, X. Meng, F. Zhang, X. Zhang, M. Ba, T. Szeto, A. Kukuljac, M. T. Marty, D. Schultz, S. Cherry, Y. Xiang, Y. Chen, J. Wang, *J. Med. Chem.* **2022**, *65*, 2848-2865.

[98] C. Ma, Z. Xia, M. D. Sacco, Y. Hu, J. A. Townsend, X. Meng, J. Choza, H. Tan, J. Jang, M. V. Gongora, X. Zhang, F. Zhang, Y. Xiang, M. T. Marty, Y. Chen, J. Wang, *J. Am. Chem. Soc.* **2021**, *143*, 20697–20709.

[99] C.-H. Zhang, E. A. Stone, M. Deshmukh, J. A. Ippolito, M. M. Ghahremanpour, J. Tirado-Rives, K. A. Spasov, S. Zhang, Y. Takeo, S. N. Kudalkar, Z. Liang, F. Isaacs, B. Lindenbach, S. J. Miller, K. S. Anderson, W. L. Jorgensen, *ACS Cent. Sci.* **2021**, *7*, 467–475.

[100] S. H. Han, C. M. Goins, T. Arya, W.-J. Shin, J. Maw, A. Hooper, D. P. Sonawane, M. R. Porter, B. E. Bannister, R. D. Crouch, A. A. Lindsey, G. Lakatos, S. R. Martinez, J. Alvarado, W. S. Akers, N. S. Wang, J. U. Jung, J. D. Macdonald, S. R. Stauffer, *J. Med. Chem.* **2022**, *65*, 2880-2904.

[101] Y. Unoh, S. Uehara, K. Nakahara, H. Nobori, Y. Yamatsu, S. Yamamoto, Y. Maruyama, Y. Taoda, K. Kasamatsu, T. Suto, K. Kouki, A. Nakahashi, S. Kawashima, T. Sanaki, S. Toba, K. Uemura, T. Mizutare, S. Ando, M. Sasaki, Y. Orba, H. Sawa, A. Sato, T. Sato, T. Kato, Y. Tachibana, *J. Med. Chem.* **2022**, *65*, 6499-6512.

[102] J. D. A. Tyndall, *J. Med. Chem.* **2022**, *65*, 6496-6498.

[103] D. Shin, R. Mukherjee, D. Grewe, D. Bojkova, K. Baek, A. Bhattacharya, L. Schulz, M. Widera, A. R. Mehdipour, G. Tascher, P. P. Geurink, A. Wilhelm, G. J. van der Heden van Noort, H. Ovaa, S. Muller, K.-P.

Knobeloch, K. Rajalingam, B. A. Schulman, J. Cinatl, G. Hummer, S. Ciesek, I. Dikic, *Nature* **2020**, *587*, 657-662.

[104] K. Ratia, A. Kilianski, Y. M. Baez-Santos, S. C. Baker, A. Mesecar, *PLoS Pathog.* **2014**, *10*, e1004113.

[105] S.-W. Li, C.-Y. Wang, Y.-J. Jou, S.-H. Huang, L.-H. Hsiao, L. Wan, Y.-J. Lin, S.-H. Kung, C.-W. Lin, *Int. J. Mol. Sci.* **2016**, *17*, 678.

[106] K. Ratia, S. Pegan, J. Takayama, K. Sleeman, M. Coughlin, S. Baliji, R. Chaudhuri, W. Fu, B. S. Prabhakar, M. E. Johnson, S. C. Baker, A. K. Ghosh, A. D. Mesecar, *Proc. Natl., Acad. Sci. U S A* **2008**, *105*, 16119-16124.

[107] A. K. Ghosh, J. Takayama, Y. Aubin, K. Ratia, R. Chaudhuri, Y. Baez, K. Sleeman, M. Coughlin, D. B. Nichols, D. C. Mulhearn, B. S. Prabhakar, S. C. Baker, M. E. Johnson, A. D. Mesecar, *J. Med. Chem.* **2009**, *52*, 5228-5240.

[108] J. Osipiuk, S.-A. Azizi, S. Dvorkin, M. Endres, R. Jedrzejczak, K. A. Jones, S. Kang, R. S. Kathayat, Y. Kim, V. G. Lisnyak, S. L. Maki, V. Nicolaescu, C. A. Taylor, C. Tesar, Y.-A. Zhang, Z. Zhou, G. Randall, K. Michalska, S. A. Snyder, B. C. Dickinson, A. Joachimiak, *Nat. Commun*. **2021**, *12*, 743.

[109] Z. Fu, B. Huang, J. Tang, S. Liu, M. Liu, Y. Ye, Z. Liu, Y. Xiong, W. Zhu, D. Cao, J. Li, X. Niu, H. Zhou, Y. J. Zhao, G. Zhang, H. Huang, *Nat. Commun.* **2021**, *12*, 488.

[110] X. Gao, B. Qin, P. Chen, K. Zhu, P. Hou, J. A. Wojdyla, M. Wang, S. Cui, *Acta Pharm Sin B.* **2021**, *11*, 237-245.

[111] Z. Shen; K. Ratia; L. Cooper; D. Kong; H. Lee; Y. Kwon; Y. Li; S. Alqarni; F. Huang; O. Dubrovskyi; L. Rong; G. R. Thatcher; R. Xiong. *J. Med. Chem.* **2022**, *65*, 2940-2955.

[112] H. Shan; J. Liu; J. Shen; J. Dai; G. Xu; K. Lu; C. Han; Y. Wang; X. Xu; Y. Tong; H. Xiang; Z. Ai; G. Zhuang; J. Hu; Z. Zhang; Y. Li; L. Pan; L. Tan. *Cell Chemical Biology*, **2021**, *28*, 855-865.

[113] B. Wang; V. Svetlov; Y. I. Wolf; E. V. Koonin; E. Nudler; I. Artsimovitch. Allosteric Activation of SARS-CoV-2 RNA-Dependent RNA Polymerase by Remdesivir Triphosphate and Other Phosphorylated Nucleotides. *mBio* **2021**, *12*, e0142321.

[114] F. Kabinger, C. Stiller, J. Schmitzová, C. Dienemann, G. Kokic, H. S. Hillen, C. Höbartner, P. Cramer, *Nat. Struct. Mol. Biol.* **2021**, *28*, 740–746.

[115] E. Eroglu, C. Toprak, *Int. J. Pharm. Sci. Res.* **2021**, *12*, 1950-1957.

[116] S. A. Olender, T. L. Walunas, E. Martinez, K. K. Perez, A. Castagna, S. Wang, D. Kurbegov, P. Goyal, D. Ripamonti, B. Balani, F. G. De Rosa, S. De Wit, S.-W. Kim, G. Diaz, R. Bruno, K. M. Mullane, D. C. Lye, R. L. Gottlieb, R. H. Haubrich, A. P. Chokkalingam, G. Wu, H. Diaz-Cuervo, D. M. Brainard, I.-H. Lee, H. Hu, L. Lin, A. O. Osinusi, J. I. Bernardino, M. Boffito, *Open Forum Infect. Dis.* **2021**, *8*, ofab278.

[117] G. Kokic, H. S. Hillen, D. Tegunov, C. Dienemann, F. Seitz, J. Schmitzova, L. Farnung, A. Siewert, C. Höbartner, P. Cramer, *Nat. Commun.* **2021**, *12*, 279.

[118] M. Y. Ghazwani; A. H. Bakheit; A. R. Hakami; H. M. Alkahtani; A. A. Almehizia. *Crystals*, **2021**, *11*, 471.

[119] C. D. Spinner, R. L. Gottlieb, G. J. Criner, J. R. Arribas López, A. M. Cattelan, A. Soriano Viladomiu, O. Ogbuagu, P. Malhotra, K. M. Mullane, A. Castagna, L. Y. A. Chai, M. Roestenberg, O. T. Y. Tsang, E. Bernasconi, P. Le Turnier, S.-C. Chang, D. SenGupta, R. H. Hyland, A. O. Osinusi, H. Cao, C. Blair, H. Wang, A. Gaggar, D. M. Brainard, M. J. McPhail, S. Bhagani, M. Y. Ahn, A. J. Sanyal, G. Huhn, F. M. Marty, for the GS-US-540-5774 Investigators. *JAMA* **2020**, *324*, 1048-1057.

[120] J. D. Goldman, D. C. B. Lye, D. S. Hui, K. M. Marks, R. Bruno, R. Montejano, C. D. Spinner, M. Galli, M.-Y. Ahn, R. G. Nahass, Y.-S. Chen, D. SenGupta, R. H. Hyland, A. O. Osinusi, H. Cao, C. Blair, X. Wei, A. Gaggar, D. M. Brainard, W. J. Towner, J. Muñoz, K. M. Mullane, F. M. Marty, K. T. Tashima, G. Diaz, A. Subramanian, *N. Engl. J. Med.* **2020**, *383*, 1827–1837.

[121] J. Grein, N. Ohmagari, D. Shin, G. Diaz, E. Asperges, A. Castagna, T. Feldt, G. Green, M. L. Green, F.-X. Lescure, E. Nicastri, R. Oda, K. Yo, E. Quiros-Roldan, A. Studemeister, J. Redinski, S. Ahmed, J. Bernett, D. Chelliah, D. Chen, S. Chihara, S. H. Cohen, J. Cunningham, A. D'Arminio Monforte, S. Ismail, H. Kato, G. Lapadula, E. L'Her, T. Maeno, S. Majumder, M. Massari, M. Mora-Rillo, Y. Mutoh, D. Nguyen, E. Verweij, A. Zoufaly, A. O. Osinusi, A. DeZure, Y. Zhao, L. Zhong, A. Chokkalingam, E. Elboudwarej, L. Telep, L. Timbs, I. Henne, S. Sellers, H. Cao, S. K. Tan, L. Winterbourne, P. Desai, R. Mera, A. Gaggar, R. P. Myers, D. M. Brainard, R. Childs, T. Flanigan, *N. Engl. J. Med.* **2020**, *382*, 2327–2336.

[122] R. M. Cox, J. D. Wolf, C. M. Lieber, J. Sourimant, M. J. Lin, D. Babusis, V. DuPont, J. Chan, K. T. Barrett, D. Lye, R. Kalla, K. Chun, R. L. Mackman, C. Ye, T. Cihlar, L. Martinez-Sobrido, A. L. Greninger, J. P. Bilello, R. K. Plemper, *Nat. Commun.* **2021**, *12*, 6415.

[123] J. Zhao, S. Guo, D. Yi, Q. Li, L. Ma, Y. Zhang, J. Wang, X. Li, F. Guo, R. Lin, C. Liang, Z. Liu, S. Cen, *Antiviral Res.* **2021**, *190*, 105078.

[124] Stanford University. *A Phase 2 Randomized, Double Blinded, Placebo Controlled Study of Oral Favipiravir Compared to Standard Supportive Care in Subjects With Mild or Asymptomatic COVID-19*; Clinical trial registration NCT04346628; clinicaltrials.gov, 2021.

[125] Fujifilm Pharmaceuticals U.S.A., Inc. *Open Label, Randomized, Controlled Phase 2 Proof-of-Concept Study of the Use of Favipiravir Compared to Standard of Care in Hospitalized Subjects With COVID-19*; Clinical trial registration NCT04358549; clinicaltrials.gov, 2021.

[126] Appili Therapeutics Inc. *Favipiravir for Patients With Mild to Moderate Disease From Novel Coronavirus (COVID-19)*; Clinical trial registration NCT04600895; clinicaltrials.gov, 2021.

[127] A. Shannon, B. Selisko, N.-T.-T. Le, J. Huchting, F. Touret, G. Piorkowski, V. Fattorini, F. Ferron, E. Decroly, C. Meier, B. Coutard, O. Peersen, B. Canard, *Nat. Commun.* **2020**, *11*, 4682.

[128] K. Naydenova, K. W. Muir, L.-F. Wu, Z. Zhang, F. Coscia, M. J. Peet, P. Castro-Hartmann, P. Qian, K. Sader, K. Dent, D. Kimanius, J. D. Sutherland, J. Löwe, D. Barford, C. J. Russo, *Proc. Natl. Acad. Sci.* **2021**, *118*, e2021946118.

[129] Merck Sharp & Dohme Corp. *A Phase 2/3, Randomized, Placebo-Controlled, Double-Blind Clinical Study to Evaluate the Efficacy, Safety, and Pharmacokinetics of MK-4482 in Non-Hospitalized Adults With COVID-19.*; Clinical trial registration NCT04575597; clinicaltrials.gov, 2021.

[130] M. Imran, M. K. Arora, S. M. B. Asdaq, S. A. Khan, S. I. Alaqel, M. K. Alshammari, M. M. Alshehri, A. S. Alshrari, A. Mateq Ali, A. M. Al-shammeri, B. D. Alhazmi, A. A. Harshan, Md. T. Alam, A. Abida, *Molecules* **2021**, *26*, 5795.

[131] R. Abdelnabi, C. S. Foo, S. J. F. Kaptein, X. Zhang, T. N. D. Do, L. Langendries, L. Vangeel, J. Breuer, J. Pang, R. Williams, V. Vergote, E. Heylen, P. Leyssen, K. Dallmeier, L. Coelmont, A. K. Chatterjee, R. Mols, P. Augustijns, S. De Jonghe, D. Jochmans, B. Weynand, J. Neyts, *EBioMedicine* **2021**, *72*, 103595.

[132] A. A. Elfiky, *J. Biomol. Struct. Dyn.* **2020**, 1–9.

[133] Q. Li, D. Yi, X. Lei, J. Zhao, Y. Zhang, X. Cui, X. Xiao, T. Jiao, X. Dong, X. Zhao, H. Zeng, C. Liang, L. Ren, F. Guo, X. Li, J. Wang, S. Cen, *Acta Pharm. Sin. B* **2021**, *11*, 1555–1567.

[134] K. Zandi, K. Musall, A. Oo, D. Cao, B. Liang, P. Hassandarvish, S. Lan, R. L. Slack, K. A. Kirby, L. Bassit, F. Amblard, B. Kim, S. AbuBakar, S. G. Sarafianos, R. F. Schinazi, *Microorganisms* **2021**, *9*, 893.

[135] K. Zandi; F. Amblard; K. Musall; J. Downs-Bowen; R. Kleinbard; A. Oo. D. Cao; B. Liang; O. O. Russell; T. McBrayer; L. Bassit; B. Kim; R. F. Schinazi. Repurposing Nucleoside Analogs for Human Coronaviruses. *Antimicrob. Agents Chemother.* **2020**, *65*, e01652-20.

[136] P. Krafcikova, J. Silhan, R. Nencka, E. Boura, *Nat. Commun.* **2020**, *11*, 3717.

[137] M. Rosas-Lemus, G. Minasov, L. Shuvalova, N. L. Inniss, O. Kiryukhina, J. Brunzelle, K. J. F. Satchell, *Sci. Signal.* **2020**, *13*, eabe1202.

[138] T. Otava, M. Šála, F. Li, J. Fanfrlík, K. Devkota, S. Perveen, I. Chau, P. Pakarian, P. Hobza, M. Vedadi, E. Boura, R. Nencka, *ACS Infect. Dis.* **2021**, *7*, 2214–2220.

[139] O. Bobiļeva, R. Bobrovs, I. Kaņepe, L. Patetko, G. Kalniņš, M. Šišovs, A. L. Bula, S. Grīnberga, M. Borodušķis, A. Ramata-Stunda, N. Rostoks, A. Jirgensons, K. Tārs, K. Jaudzems, *ACS Med. Chem. Lett.* **2021**, *12*, 1102–1107.

[140] R. Ahmed-Belkacem, M. Hausdorff, A. Delpal, P. Sutto-Ortiz, A. M. G. Colmant, F. Touret, N. S. Ogando, E. J. Snijder, B. Canard, B. Coutard, J.-J. Vasseur, E. Decroly, F. Debart, *J. Med. Chem.* **2022**, *65*, 6231–6249.

[141] P. C. Taylor, A. C. Adams, M. M. Hufford, I. de la Torre, K. Winthrop, R. L. Gottlieb, *Nat. Rev. Immunol.* **2021**, *21*, 382-393.

[142] X. Hu, C. Z. Chen, M. Xu, Z. Hu, H. Guo, Z. Itkin, P. Shinn, P. Ivin, M. Leek, T. J. Liang, M. Shen, W. Zheng, M. D. Hall, *ACS Med. Chem. Lett.* **2021**, *12*, 1267–1274.

[143] D. Bojadzic, O. Alcazar, J. Chen, S.-T. Chuang, J. M. Condor Capcha, L. A. Shehadeh, P. Buchwald, *ACS Infect. Dis.* **2021**, *7*, 1519–1534.

[144] M. R. Straus, M. K. Bidon, T. Tang, J. A. Jaimes, G. R. Whittaker, S. Daniel, *ACS Infect. Dis.* **2021**, *7*, 2807–2815.

[145] X. Hu, C. Z. Chen, M. Xu, Z. Hu, H. Guo, Z. Itkin, P. Shinn, P. Ivin, M. Leek, T. J. Liang, M. Shen, W. Zheng, M. D. Hall, *ACS Med. Chem. Lett.* **2021**, *12*, 1267-1274.

[146] *Kinase Inhibitors*. COVID-19 Treatment Guidelines. https://www.covid19treatmentguidelines.nih.gov/therapies/immunomodulators/kinase-inhibitors/.

[147] W. Zhang, Y. Zhao, F. Zhang, Q. Wang, T. Li, Z. Liu, J. Wang, Y. Qin, X. Zhang, X. Yan, X. Zeng, S. Zhang, *Clin. Immunol.* **2020**, *214*, 108393.

[148] O. Melikhov, T. Kruglova, K. Lytkina, G. Melkonyan, E. Prokhorovich, G. Putsman, G. Rodoman, A. Vertkin, A. Zagrebneva, J. Stebbing, *Ann. Rheum. Dis.* **2021**, *80*, 1245-1246.

[149] P. Richardson, I. Griffin, C. Tucker, D. Smith, O. Oechsle, A. Phelan, M. Rawling, E. Savory, J. Stebbing, *Lancet* **2020**, *395*, e30-e31.

[150] Research, C. for D. E. and. *Coronavirus (COVID-19) | Drugs*. FDA. https://www.fda.gov/drugs/emergency-preparedness-drugs/coronavirus-covid-19-drugs.

[151] A. C. Kalil, T. F. Patterson, A. K. Mehta, K. M. Tomashek, C. R. Wolfe, V. Ghazaryan, V. C. Marconi, G. M. Ruiz-Palacios, L. Hsieh, S. Kline, V. Tapson, N. M. Iovine, M. K. Jain, D. A. Sweeney, H. M. El Sahly, A. R. Branche, J. Regalado Pineda, D. C. Lye, U. Sandkovsky, A. F. Luetkemeyer, S. H. Cohen, R. W. Finberg, P. E. H. Jackson, B. Taiwo, C. I. Paules, H. Arguinchona, N. Erdmann, N. Ahuja, M. Frank, M. Oh, E.-S. Kim, S. Y. Tan, R. A. Mularski, H. Nielsen, P. O. Ponce, B. S. Taylor, L. Larson, N. G. Rouphael, Y. Saklawi, V. D. Cantos, E. R. Ko, J. J. Engemann, A. N. Amin, M. Watanabe, J. Billings, M.-C. Elie, R. T. Davey, T. H. Burgess, J. Ferreira, M. Green, M. Makowski, A. Cardoso, S. de Bono, T. Bonnett, M. Proschan, G. A. Deye, W. Dempsey, S. U. Nayak, L. E. Dodd, J. H. Beigel, *N. Engl. J. Med.* **2021**, *384*, 795–807.

Entry for the Table of Contents

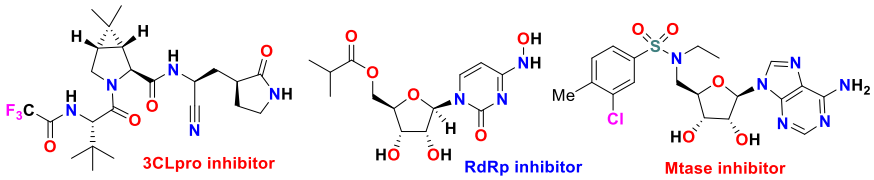

The present review *provides* an overview of *recent* drug design and medicinal chemistry efforts on small molecule drug discovery for treatment of COVID-19. The review also highlights development of nirmatrelvir that targets viral protein synthesis and remdesivir and molnupiravir that target viral RdRp. These drugs are now FDA approved therapies for the treatment of COVID-19.